EXPERIMENTAL ANALYSIS OF PASSIVE ACOUSTIC EMISSION, IN PARTICULAR THE KAISER EFFECT, UNDER DYNAMIC STRESS CONDITIONS. EXPLORING THE IMPLICATIONS FOR IN-SITU FAILURE MONITORING IN UNDERGROUND MINES.

A thesis submitted to the Delft University of Technology in partial fulfilment of the requirements for the degree of

Master of Science in Applied Earth Science

by

Luuk Mulder

August 2019

Luuk Mulder: *Experimental analysis of passive acoustic emission, in particular the Kaiser Effect, under dynamic stress conditions. Exploring the implications for in-situ failure monitoring in underground mines.* (2019)

The work in this thesis was made in the:

Applied Earth Sciences
Faculty Civil Engineering and Geosciences
Delft University of Technology

Supervisors:	Dr. Auke Barnhoorn
	Dr. Mike Buxton
	Dr. Anne-Catherine Diedonné
Co-reader:	Dr. Robrecht Schmitz

ABSTRACT

Irreversible damage induced by stress in brittle rock is accompanied by the formation of micro-cracks. The strain energy released during the fracturing process is released in the form of acoustic emission. This thesis applied the non-intrusive method of acoustic emission monitoring to assess the deformation process of brittle rock during cyclical loading and loading to failure in a standard uniaxial compressive strength test set-up. It is confirmed that the stress-strain curve is clearly separated into five phases and that the cumulative hits recorded throughout the failure process correspond with these five phases. Furthermore it is found that there is an obvious rise in trend in the amplitude of the acoustic events as the rock nears failure, but that individual events of high amplitude should not be considered indicative for the damage in the rock. Additionally it is found that high amplitudes characteristic for near failure stress are recorded at 25% of the failure stress if the rock has been under high stresses, indicating a change in fracture mode. The Kaiser Effect, the phenomenon defined as the absence of detectable acoustic emission events until the load imposed on the material exceeds the previous applied level, was confirmed during uniaxial cyclical loading. Through loading samples from a highly stressed pillar in the Nepheline Syenite Stjernoya Mine in Norway, it is found that the onset of acoustic emission may be indicative of the stress in the pillar. These findings are useful to further develop acoustic emission as a monitoring method in a range of applied earth science applications.

ACKNOWLEDGEMENTS

I would like to thank Karel Heller for his support during the assembly of the Richter System. Wim verwaal for the support with the UCS system and Marc Friebel for further support in the Lab. My father for helping me out with his 3D printer. I would further like to thank Robrecht Schmitz and Sibelco for the inspiration to do this research and for providing the samples from the Stjernoya Mine. Lastly I would like to thank Mike Buxton and Auke Barneveld; Mike for the interesting meetings and discussion from a mining perspective and Auke for both his academic support and his coaching throughout my research.

...

CONTENTS

1 INTRODUCTION

Due to the developments in modern electronics, complex monitoring systems to monitor the progressive damage in rocks have become more and more feasible. Monitoring the passive acoustic emissions is one of such methods. Recording and analysing acoustic emission is used as a non-intrusive method for studying and monitoring the damage process in materials such as rock, concrete, composites or metals under stress Pappas et al. [1998], Loutas and Kostopoulos [2009], Hardy [2005],Sheng et al. [2019], Cox and Meredith [1993], Young and Martin [1993], Mclaskey et al. [2010] or for monitoring processes which purposefully induce damage such as hydraulic fracturing Li et al. [2019], borehole monitoring Hu et al. [2018] or water jet drilling Sheng et al. [2019]. The reason that acoustic emission can be used as a method for damage monitoring in materials is that stress induced irreversible deformation in brittle and semi brittle materials is accompanied by microfracturing. A fraction of the strain energy released during this fracturing process is released in the form of transient stress waves, known as acoustic emission. This acoustic emission can be recorded by sensors such as a piezoelectric transducer, making it possible to monitor the acoustic emission released during the deformation process of a material. Since the damaging process is irreversible (at least on the short term), the process is cumulative and can therefore be monitored as such Cox and Meredith [1993].

The different phases of deformation of brittle rock have been studied by many researchers Hoek [1965], Bieniawski [1967], Brace et al. [1966], and Nicksiar and Martin [2014] gives a conclusive account of the deformation of granite and the related acoustic emission. It has been found that the stress-strain curve is clearly separated into five phases; from unstressed rock to rock failure. These five phases in the stress-strain curve can similarly be recognised in the release of acoustic emission. An overview of the five phases including their acoustic response in terms of hits recorded is shown in figure 1.1.

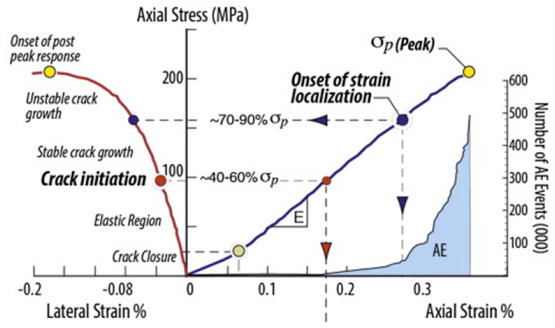

Figure 1.1: Phases of deformation in brittle rock, showing the axial- and radial strain as well as the cumulative hits recorded during a uniaxial compressive test, based on Nicksiar and Martin [2014]

Additional to the correspondence with the phases of deformation in brittle rock another curiosity related to acoustic activity has been observed; the Kaiser Effect. The Kaiser effect is the phenomenon defined as the absence of detectable acoustic emission events until the load imposed on the material exceeds the previous applied level [Li and Nordlund, 1993] and was first observed in tensile tests on metals by Kaiser [1950]. The Kaiser effect in rocks is similarly observed in the lab. The

schematic graph in figure 1.2 visualises the manifestation of the Kaiser Effect occurring during two loading cycles. The occurrence of the Kaiser Effect in brittle rock has been observed by many Lavrov [2003], Holcomb [1993], Li and Nordlund [1993], Kallimogiannis et al. [2017]. The retrieval of the stress history of a rock through stress memory is considered one of the potential uses of the Kaiser Effect Holcomb [1993], Lavrov [2003], Lehtonen et al. [2012], Momayez and Hassuni [1992],, Hughson and Crawford [1986]. Using the Kaiser Effect to retrieve the in-situ stress from a collected sample through uniaxial testing comes with complications since the uniaxial compression is not reflective of the in-situ situation Holcomb [1993], additionally the direction of the uniaxial testing cannot deviate more than 10°from the direction of the stress to be retrieved.

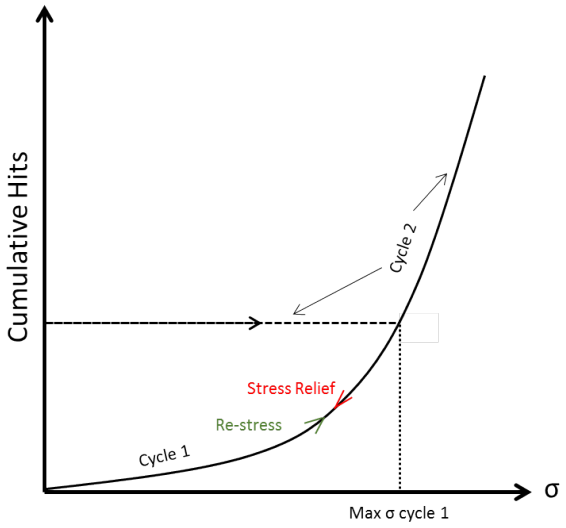

Figure 1.2: A schematic graph of the stress vs the cumulative acoustic events or 'hits' recorded in two cycles under uniaxial compression

This research aims to use the new Richter system, a newly acquired piece of equipment at the faculty of Geosciences and Civil Engineering; a multi channel device which can record and process acoustic events. The acoustic data acquired is used to confirm the occurrence of the Kaiser effect and to analyse the acoustic events in terms of cumulative hits as well as the maximum amplitude recorded per acoustic event and relate it to the progressive failure of brittle rock. Then finally to research the potential for acoustic monitoring, combining both the findings regarding the Kaiser Effect as well as regarding the different phases of deformation. These goals are pursued through two types of experiments performed in the uniaxial compressive test set-up; cyclical loading and loading to failure. These two tests are performed on samples collected from two blocks from the Stjernoya mine in Norway; one block of ore and one block collected from a highly stressed pillar.

2 KAISER-EFFECT

2.1 THE SOURCE OF THE KAISER EFFECT

As a poly-crystalline medium such as a rock is under non-hydrostatic stress, e.g. during the deformation of mine pillars, local tensile stresses within the rock are generated on a micro scale. Brace et al. [1966], Bieniawski [1967] These local tensile stresses are there due to local material mismatches such as differences in grain size and contact stresses caused by irregularities in the grain boundaries of different grains. Diederichs et al. [2004], Kranz [1983]. These local tensile stresses initiate the formation of microcracks. Lockner [1993]. As a result a microcrack will develop to maintain equilibrium. The microcracks grow by small jumps to the next equilibrium position, releasing part of the strain energy in the for of elastic transient waves. Sayers and Kachanov [1995] [Costin, 1983]. The Kaiser effect is the phenomenon defined as the absence of detectable acoustic emission events until the load imposed on the material exceeds the previous applied level [Li and Nordlund, 1993] and was first observed in tensile tests on metals by Kaiser [1950], a visualisation of the manifestation of the kaiser effect during a cyclical experiment is shown in figure 2.1. The Kaiser effect is instigated as the damage surface, defined by the stresses previously applied to the medium, is reached and surpassed by continued loading leading to new crack growth with associated acoustic emissions, until the next equilibrium position is reached. Holcomb [1993]

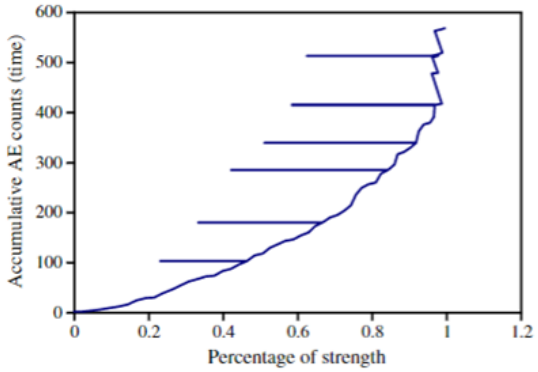

Figure 2.1: The manifestation of the Kaiser effect during experiments by Lehtonen et al. [2012]

2.2 LIMITATIONS OF STRESS MEASUREMENT USING THE KAISER EFFECT

From the moment the Kaiser effect was discovered, it has been considered to be a potential method for finding the stress history of a material. It was widely believed that through applying stress uniaxially the complete stress history of the material of a rock could be retrieved, however a full understanding of the triaxial state of stress play an elemental role for a correct application of the Kaiser effect for retrieving the stress history of a rock [Holcomb, 1993]. Even in the simple case of uniaxial loading,

acoustic activity starts before exceeding the previously applied stress.This activity is possibly caused by frictional movement along existing cracks [Lavrov, 2003]. It is found that to obtain a well pronounced Kaiser effect the load applied to the rock should range from 30% to 80% of the peak strength of a rock Lavrov [2003]. The reason for this is that this coincides with the range on the stress-strain curve from the crack initiation threshold to the crack damage threshold as discussed in chapter 3.

In experiments executed by [Michihiro et al., 1992] stress is applied on a rock in three cycles in which $\sigma_I^{III} > \sigma_I^I > \sigma_I^{II}$. The tests demonstrated that if the rock was held at σ_I^{II} until strain recovery finished. The Kaiser effect of the third cycle was observed at the stress of the second cycle rather than the first one. Therefore it cannot be blindly assumed the rock properly 'memorises' its' stress history. This consequently has a big impact on the possibility of stress measurements through the Kaiser effect method.

For brittle rocks the effect of the time duration of the application of stress on the Kaiser effect has been observed to be insignificant. [Lavrov, 2003] The influence of time delay on the Kaiser effect has been observed to be much more significant. However the discrepancy of the results of different researchers is quite large. Two research teams have had observed very different results when doing research on the Kaiser effect in a granite; one team found the Kaiser effect to be well-observed after a 300-day period whilst another research team also researching a granite found that the Kaiser effect was completely lost after a 20 day time period.

The coring process during which the cores used to obtain AE data and the Kaiser effect can be limiting to the reliability as well as the presence of the Kaiser Effect. Several elements in the coring process may play a role, these were summarised by [Lehtonen et al., 2012]:

1. Stress is a second order tensor quantity which requires six independent quantities for its specification. Therefore it is required to collect a core in all 6 directions, however drilling the cores itself will exert stress affecting the stress history of the rock.

2. Additionally to the damage done during the core drilling process, the actual stress applied to the rock has now been removed. Applying an unconfined stress will not resemble the in situ stresses. This will affect the behaviour of the sample.

3. The moment the core is drilled from the rock mass the stress is relieved and this will affect the microcracks, as mentioned in more detail by [Lavrov, 2003].

4. Generally the experiments executed are not done on site, therefore during transport and storage the samples are not protected from the environment, which has unknown effect on the samples, due to drying or exposure to water.

5. It is important to investigate how representative the core sample is of the rock mass or object within the rock mass that is being researched.

2.2.1 Directional sensitivity of the Kaiser effect

In the lab, the principal stresses are always known, however in the field, it is near impossible to determine the principal stresses. In some situations it can be based on the geology or on common sense, however in underground excavations, with an ever-changing structure and stress distribution, the principal stress is difficult to estimate and therefore estimations are often inaccurate. Thus for finding the stress history of a rock it is important to know what the impact is of deviation from the principal stress on the Kaiser effect. An experiment was performed by [Holcomb and Costin, 1986] on granite for which stress was first applied on a large block after which cores were collected from the block for further testing. The experiment

demonstrated that the Kaiser effect is lost very quickly when the direction of the stress applied on a core deviates from the stress applied on the large sample. The Kaiser effect was detected only up to a deviation of 10°. This implies that determination of the stress history is very difficult. However in a situation where several stress situations have existed in the same rock, the Kaiser effect could be used to retrieve the stresses that have existed in different directions. This has the potential to be very informative if the direction and location of the sample collected are known. Lehtonen et al. [2012] however was able to find the in-situ stress relatively recently and concluded that using the Kaiser Effect as a method to determine the in-situ stress is an enigma. Numerous complications are involved using the method however several researchers have been able to determine the in-situ stress correctly, including Lehtonen et al. [2012] himself.

2.2.2 Kilometre-scale Kaiser effect

The manifestation of the kaiser effect has not only been researched in the lab. Heimisson et al. [2002] observed the manifestation of the Kaiser Effect on kilometre scale in the Krafla volcano in Iceland. During the first volumetric change high seismic activity is recorded and the seismicity correlates well with the volumetric inflation. In the following cycles seismic activity is very low until the previous cycle is exceeded and an abrupt increase in seismicity is observed. The manifestation is especially clear in the first three cycles shown in figure 2.2. It is theorised by Heimisson et al. [2002] that the decrease in clarity of the Kaiser Effect in the later years is due to 5 earthquakes occurring in the area, completely altering the stress field.

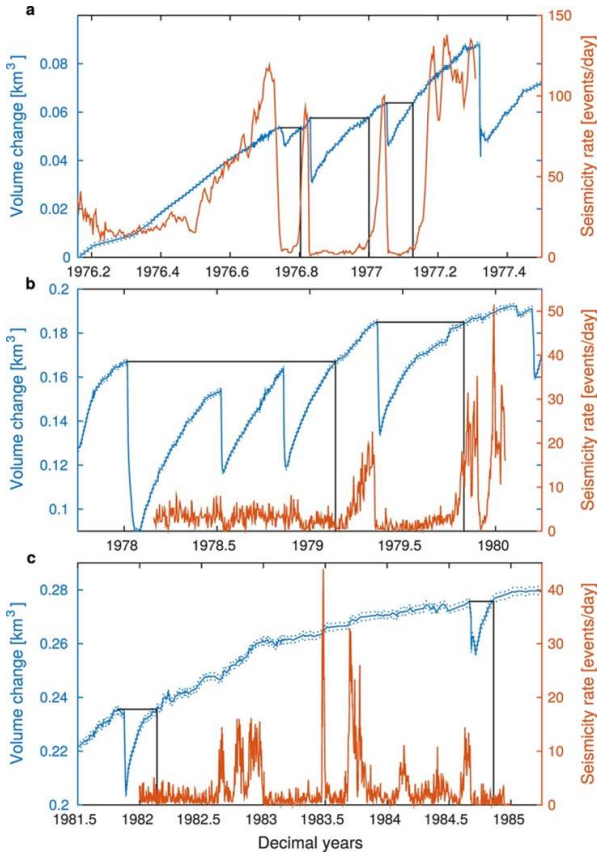

Figure 2.2: The occurrence of the Kaiser effect in kilometre scale in the Icelandic volcano, the Krafla volcano

3 THE BEHAVIOUR OF BRITTLE ROCK UNDER COMPRESSIVE STRESS

3.1 FRACTURE MECHANICS OF BRITTLE ROCK

Since the Kaiser effect and stress related acoustic emission in rock are connected to the formation of microcracks during the deformation of a rock, it is important to discuss fracture mechanics and the process of deformation. The field of fracture mechanics can be said to have started with the theory by Inglis [1913], who found a solution for the stress field around an ellipse. Griffith [1920] used the findings of Inglis for an energy-balance approach for his theory of fracture mechanics.

3.1.1 Inglis' Stress Concentrators

Elemental to the development of the Griffith's theory was the stress analysis by Inglis of an elliptical void in an uniformly stressed plate. Inglis' analysis showed that the local stresses at the tip of a void could be several times higher than the applied stress. As descibed by Inglis a plate subjected to uniformly applied stress σ_A containing an elliptical void, of height $2b$ and length $2c$ is shown in figure 3.1

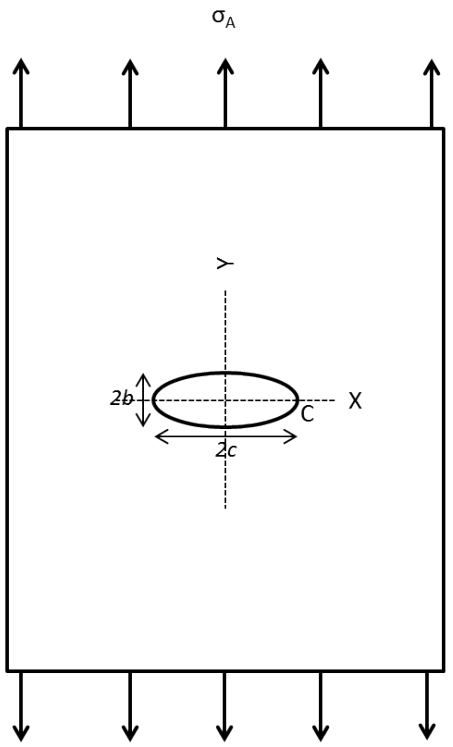

Figure 3.1: Plate containing elliptical void, subject to uniform stress σ_A. C denotes the tip of the void, interpretation from Lawn [1993]

The boundary of the elliptical void within the plate is given by:

$$\frac{x^2}{c^2} + \frac{y^2}{b^2} = 1$$

The radius of curvature at the tip of the void, i.e. point C, in the case of $b < c$:

$$\rho = \frac{b^2}{c}$$

Point C is also the point of maximum stress concentration:

$$\sigma_C = \sigma_A(1 + \frac{2c}{b}) = \sigma_A(1 + 2\sqrt{\frac{c}{\rho}})$$

In the case of $b << c$, this reduces to

$$\frac{\sigma_C}{\sigma_A} \simeq 2\sqrt{\frac{c}{\rho}}$$

The ratio $\frac{\sigma_C}{\sigma_A}$ is an elastic stress-concentration factor. It can be immediately deduced that the concentration of stress depends on the shape of the void rather than the size. However in practice these findings did not comply with the reality, as large cracks tend to propagate easier than small cracks, violating the size-independence.

3.1.2 Griffith's theory of crack mechanics

Griffith modelled a static crack as a reversible thermodynamic system and stated that in a linear elastic material, brittle fracture initiation starts with tensile stresses at the crack tips of thin cracks inherently present within an otherwise isotropic material. Griffith looked for a setting in which the total free energy in a system would be minimised; the crack would then be on the verge of propagation. This means that crack extension occurs if the surface energy associated with the inter molecular forces at the interfaces along the crack path equal the net reduction in strain energy:

$$W = W_e + W_s$$

where W is the total potential energy, W_e is the stored elastic strain energy and W_s is the surface energy per unit area of the crack surface. This means that an increase in stress around a Griffith crack can be balanced by an in increase in strain energy, an increase in the crack surface or through the combination of both. The strain energy and and the surface area can be calculated as:

$$W_e = \frac{\pi a^2 \sigma_t^2}{E'}$$

and,

$$W_s = 4\gamma a$$

Where σ_t is the applied uniaxial tensile stress required for crack propagation, E' is Young's modulus in plane stress (thin plates) and $E/(1-\nu^2)$ in plane strain ('thick' plates), γ is the surface energy per unit area of the crack surface and a is the fracture's half length. Solving for σ_t, it is established that crack extension occurs when:

$$\sigma_t \geq \sqrt{\frac{2E'\gamma}{\pi a}}$$

Hoek [1965] showed that the Griffith theory is a reliable theory for the prediction of the initiation of a single fracture but cannot explain the failure of a rock.

3.1.3 The Hoek-Brown criterion

Hoek and Brown used the Griffith theory as a basis for their development of an empirical approximation of failure of intact rock that fit shear failure conditions for brittle rock under triaxial conditions. The following equation represents their findings.

$$\sigma_1 = \sigma_3 + \sigma_c \sqrt{m_i \frac{\sigma_3}{\sigma_c} + 1}$$

The focus of the research was on confined shear failure, assumed to be the controlling factor controlling the stability of small slopes and shallow tunnels. The tensile strength of the rock was at the time not taken into account and was often assumed to be zero. Over time the depth of excavations in civil and mining engineering, oil exploration and oil recovery increased. Depths at which the tensile strength of a rock plays a more important role. Specifically the manifestation of brittle fracture resulting in splitting, popping, spalling and rockbursts in pillars and tunnels and breakouts occurring in boreholes are tensile fracture processes. Since the findings by Hoek and Brown largely through numerical approaches several theories crack initiation and propagation have been developed.

In a review on fracture initiation and propagation in intact rocks of low porostiy, Hoek and Martin [2014] concluded the Griffith provides a simplified model, based on the initiation of fractures at inclined flaws, namely grain boundaries in the sliding crack model. Discrete Element method numerical approximation has shown that the force chain crack model is a viable alternative to describe the tensile fracture initiation coalition, fracture coalescence, spalling and the final shearing of the specimens at higher confining stresses. The force chain crack model is further explained in the next section.

3.1.4 Linear Elastic Fracture Mechanics Approach

Griffith's theory led to the development of Linear Elastic Fracture Mechanics (LEFM). The LEFM distinguishes three modes of crack loading. Mode I (opening mode), in essence normal separation of the crack walls through pure tensile opening; Mode II (sliding mode), longitudinal shearing of the crack walls in a direction normal to the crack tip and Mode III (tearing mode), lateral shearing to the tip of the crack. These three modes are visualised in 3.2 . Of these three modes, Mode I is the most relevant to crack propagation highly brittle solids such as rocks Lawn [1993] and is therefore also expected to be the most prevalent mode of cracking in the experiments performed by the researcher. These three models were used by [Atkinson, 1987] to summarise the basic foundations of LEFM:

1. A crack tip has a stress intensity factor, K_I, K_{II} or K_{III} dependent on the mode, which corresponds to the induced stress at the crack tip.

2. The material surrounding the crack has a critical stress intensity, K_{IC}, corresponding to the strength of the material surrounding the crack tip.

3. The criterion for crack propagation is:

$$K_I = K_{IC}$$

4. The crack continues to propagate as long as the above expression is met and won't stop propagating until:

$$K_I < K_{IC}$$

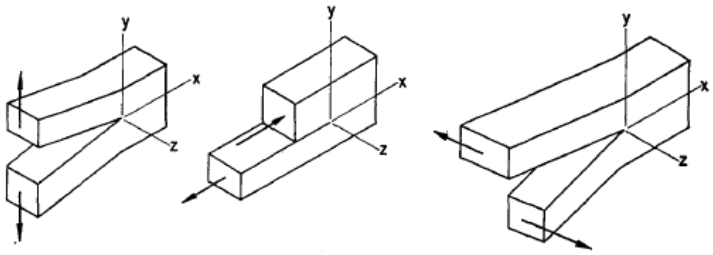

Figure 3.2: The three basic modes of crack surface displacement

3.1.5 Crack Models in Compression Loading

Two basic models, essentially more detailed variations on mode I fracturing, which are used to describe the observation of crack initiation being oriented around 15 degrees to the loading direction are the sliding-crack model proposed by and the force chain model Nicksiar and Martin [2014]. A schematic visualisation of these two models is shown in figure 3.3, which demonstrates the fundamental difference between these two models. For the sliding-crack model, a suitably oriented weak plane must be present along which sliding sliding must occur before the local tensile stresses are high enough to initiate and propagate the fractures parallel to the compressive stress. Essentially this means that the sliding-crack model is valid in case the shear stress on the crack surface is equal to the shear strength of the cracks (τ) which is defined as

$$\tau = C + \sigma_n \tan\phi$$

where C and ϕ are the cohesion and internal friction angle and σ_n is the normal stress acting on the crack surface. The force-chain crack model does not need this pre-existing weak plane to be present for the initial sliding to occur and will cause cracking provided that the normal stress on the crack surface exceeds the tensile strength. The initial heterogeneity of the mechanical and mineralogical properties of the present minerals will create local tensile stresses sufficient to form cracks.

Further research done by modelling crack initiation for different grain sizes and grain size distributions using a discrete element numerical approach indicated that crack initiation in low porosity rocks appears to be a tensile mechanism, well explained through the force chain method and that shear cracking along grain boundaries is only a prominent mechanism near peak strength.

3.2 THE FAILURE PROCESS OF BRITTLE ROCK UNDER COMPRESSIVE STRESS

The source of the registered acoustic emission of a material under stress is the formation of microcracks during deformation of the rock under stress Lavrov [2003], Lehtonen et al. [2012], Hughson and Crawford [1986]. Therefore in order to understand the nature of acoustic emission, it is essential to understand the deformation process of brittle rock. The failure process of brittle rock has been researched by many researchers. The deformation of brittle rock has been studied by many researchers Hoek [1965], Bieniawski [1967], Brace et al. [1966] and Martin [1993] gives a conclusive account of the deformation of granite and the related acoustic emission. It has been found that the deformation process of brittle rock can be delimited into 5 stages that occur during the failure process. These stages are visualised in 3.4. The five stages as stated in the figure are:

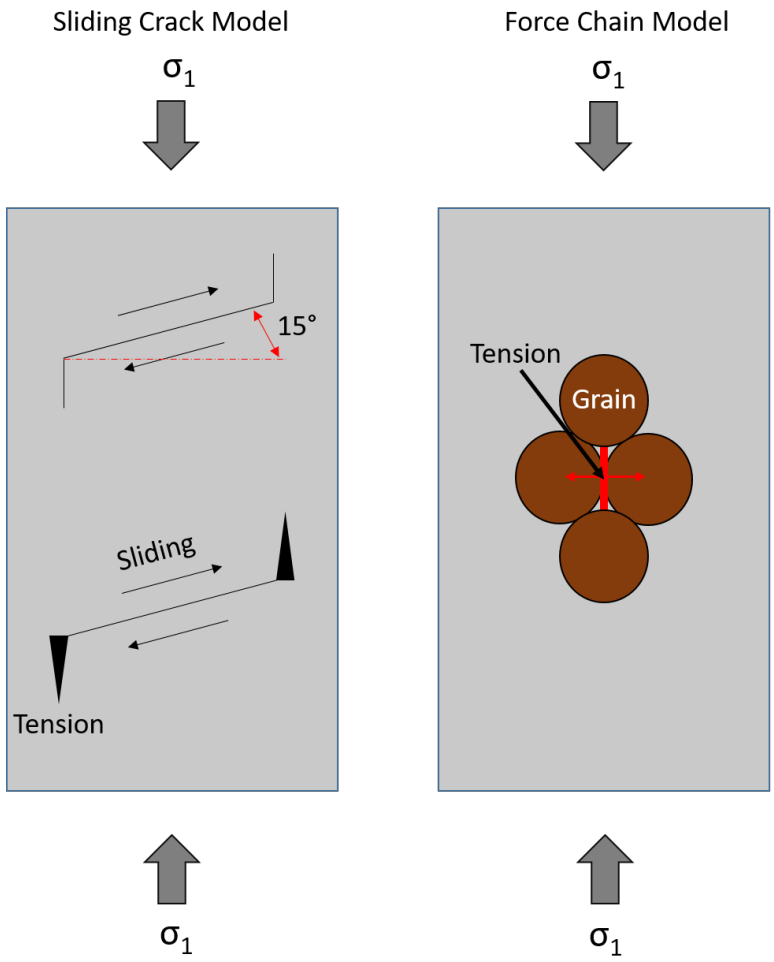

Figure 3.3: Two models commonly used to explain crack initiation observed in laboratory tests interpreted from Nicksiar and Martin [2014]

I Crack closure

II Linear elastic deformation

III Crack initiation and stable crack growth

IV Unstable crack growth

V Failure

The first stage delimited in the stress-strain curve visualised in 3.4 represents the stage during which preexisting cracks close. This point is determined through recognising the change from the stress strain curve where the axial strain changes from non-linear to linear behaviour. Once the preexisting cracks have closed the rock enters the second stage. During this stage, the rock is presumed to behave as a linearly, elastic, homogeneous material, throughout this stage Hooke's law is valid and the rock's stiffness is described by the Young's Modulus; $E = \frac{\sigma(\epsilon)}{\epsilon}$ where $\sigma(\epsilon)$ is the stress applied in the direction of the strain and ϵ the strain, or proportional deformation. The regions III to V represent the different stages of crack formation and permanent deformation of the rock

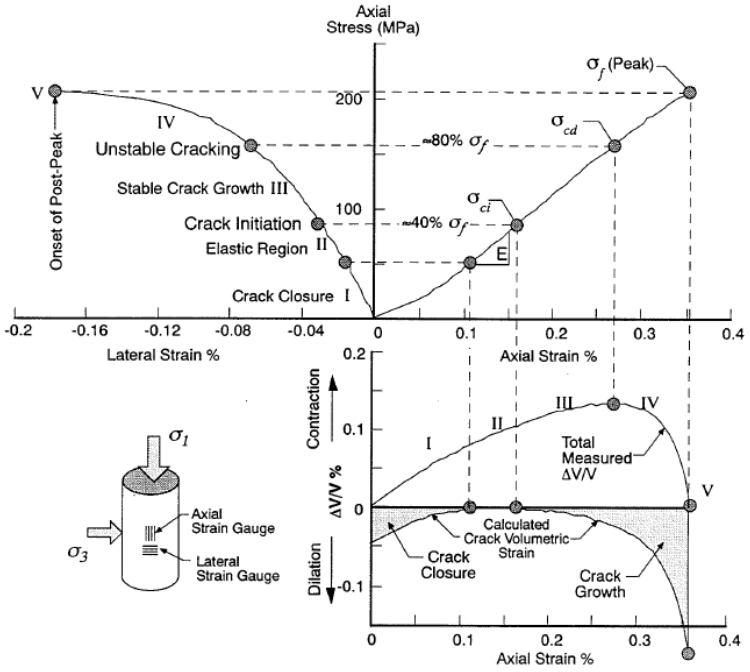

Figure 3.4: A stress-strain curve from a uniaxial compression test of Lac du Bonnet granite [Martin, 1993]

3.2.1 Stage III: Crack Initiation and Stable Crack Growth

The point at which crack initiation starts is defined as the point at which the lateral strain curve stops being linear.

Martin [1993] suggested using calculated crack volumetric strain to identify crack initiation. The crack volumetric strain is calculated by using the Young's modulus and Poisson's ratio, found during the elastic phase of the material. The elastic constants are then used to find the elastic volumetric strains by

$$\epsilon_{Velastic} = \frac{1-2\nu}{E}\sigma_{axial}$$

where E is Youngs Modulus and ν is the poissons ratio. The volumetric strain is given by:

$$\epsilon_V = \epsilon_{axial} + 2 * \epsilon_{lateral}$$

The volumetric strain attributed to cracking can be calculated by subtracting the elastic volumetric strain from the total volumetric strain.

$$\epsilon_{Vcrack} = \epsilon_V - \epsilon_{elastic}$$

Martin [1993] then defines the crack initiation as the stress level at which an increase in crack volume occurs due to dilation, similar definitions are given by **?**, Atkinson [1987] and Hoek and Martin [2014]. In further analysis of the deformation of rock, the crack volume stiffness is used. The crack volume stiffness is the the change of the slope of the crack volume strain.

3.2.2 Stage IV: Unstable Crack Growth

The onset of stage IV is defined by the axial stress level at which the volumetric strain reverses from contraction to dilation and represents commencement of unstable crack growth as defined by [Bieniawski, 1967]. At this point the stress-strain graph becomes non-linear and usually occurs at an axial stress of 70 to 85% of the peak strength. The strain hardening that occurs at the initiation of stage IV is only temporary [Martin, 1993] and the rock will fail after long term loading at this stress level. This stress level is referred to as the crack damage stress (σ_{cd}). The most significant changes during stage IV is the density of microcracks increasing by about sevenfold. This is confirmed by the dramatic increase of acoustic emission beyond σ_{cd}.

3.2.3 Stage V: Failure and Post-Peak Behaviour

Post- behaviour starts after failure of a rock at it's peak strength (σ_f). After peak strength the lateral and axial strain show a strong descent and indicate continuing dilation. In this stage the sliding initiated at the crack damage stress changes into a through-going shear zone.

4 ACOUSTIC EMISSION

During the initiation and propagation of a crack in stable crack formation, the stress applied on the material exceeds the strain energy. The rapid release of energy during fracturing is partially dissipated in the form of a transient elastic wave. In a laboratory set-up these waves are typically referred to as acoustic emission. A schematic drawing of the occurrence of an acoustic event resulting from crack propagation in a sample under stress conditions is given in figure 4.1. Acoustic emission is regarded to be similar to microseismicity, where microseismicity refers to similar elastic waves induced in the field at an engineering scale (e.g. rockbursts in mines) Ishida et al. [2017]. Due to the developments in modern electronics, specifically an increase in computer (random-access) memory and compact sensors, highly sensitive continuous monitoring of these signals is now possible.

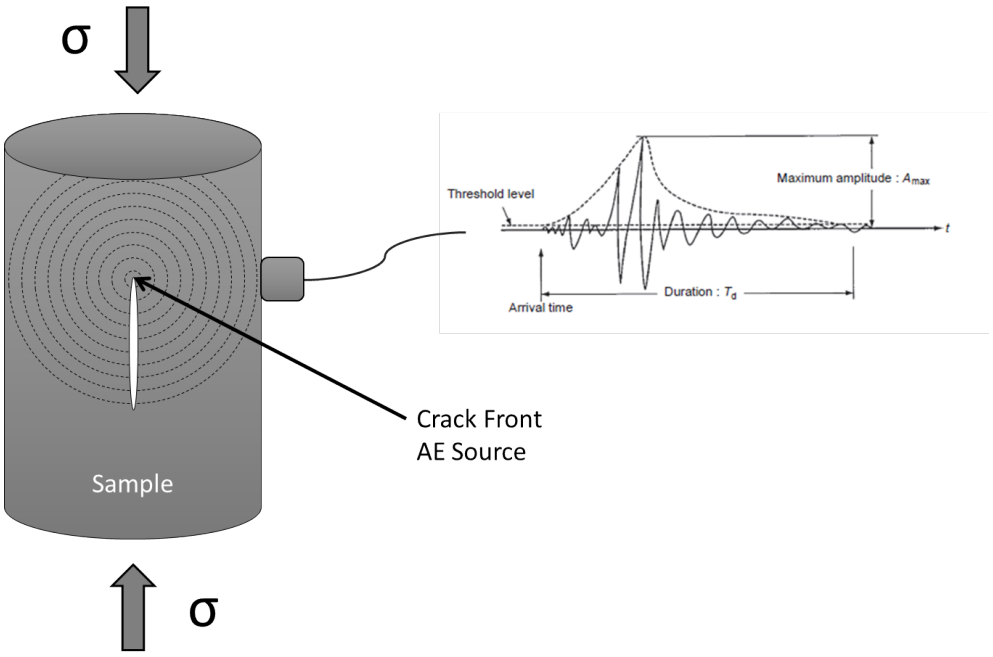

Figure 4.1: Acoustic emission from a crack propagation source

Acoustic emission is used as a non-intrusive method for studying and monitoring the damage process in materials. The monitoring of acoustic emission differs from other non-intrusive methods since the source of the signal originates from the material itself and not from an external source, additionally acoustic emission detects physical change rather than existing discontinuities. The characteristics of the recorded acoustic events can be used for damage analysis of the rock. This research focuses on two characteristics of acoustic emission; cumulative hits recorded and the maximum amplitude of each event recorded.

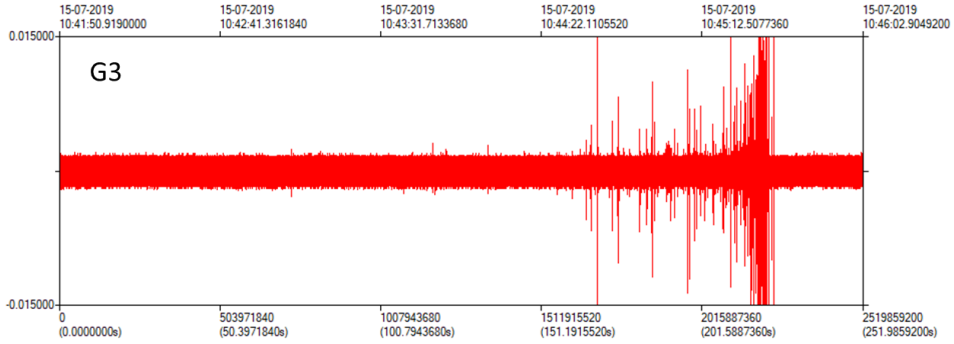

Figure 4.2: Continuous recording of sample G3 loaded to failure

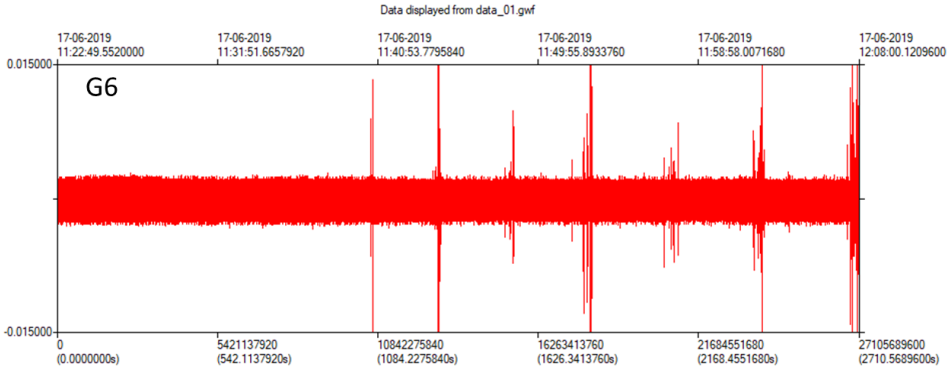

Figure 4.3: Continuous recording of sample G6 loaded cyclically

4.1 AN ACOUSTIC EVENT

A continuous recording of acoustic activity of a stressed rock sample consists of a continuously present background noise with acoustic events intermittently dispersed through. A visualisation of the full continuous recording of a sample loaded to failure and a cyclically loaded sample is given in figure 4.2 and 4.3. The intermittently dispersed acoustic events are individual occurrences. A schematic representation of a typical singular event, referred to as an acoustic event or 'hit' in this research is given in figure 4.4

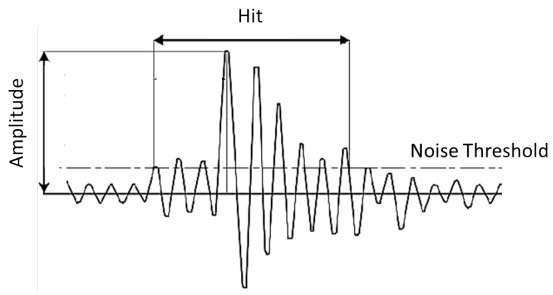

Figure 4.4: Schematic representation of an acoustic event

4.2 CUMULATIVE HITS

The initiation and propagation of cracks is the source of acoustic emission and can be assumed to be irreversible of nature, implying that the damage in the rock is of cumulative nature too Cox and Meredith [1993]. This makes counting cumulative

hits a representative form of damage analysis in rocks. The method of hit counting is based simply on the waveform exceeding a pre-set amplitude threshold just above the background noise level and therefore exclusively looks at the number of hits and does not distinguish between high and low energy events. Thompson et al. [1999] found a clear increase in 'hits' of acoustic emission during the transition from stable to unstable crack growth and many have shown an exponential increase in cumulative hits as the sample approaches failure Villaescusa et al. [2002], Martin [1994], Lavrov [2003]. Thompson et al. [1999] even used the acoustic feedback as a control for the application of stress during uniaxial compression in the lab. These results implied a clear relationship between the acoustic hits recorded and the mechanical behaviour, specifically the radial strain, of the rock. Furthermore researchers, such as Nicksiar and Martin [2013], Nicksiar and Martin [2014] and Eberhardt et al. [1998] have used the cumulative hits as a tool to confirm the five phases of deformation discussed in 3.

4.3 AMPLITUDE

The energy of the amplitude is dependent on the energy released and can be informative of the source of the acoustic event. Following the Griffith theory the energy released of a singular crack is proportional to the stress applied and the length of the crack and the surface tension of the fracture zone, i.e. the material to be fractured. Similar implications have been confirmed by several researchers; Zang et al. [1996], as well as Thompson et al. [1999] found that there is a clear increase in number of high amplitude acoustic events approaching failure. Baud and Meredith [1997] found that there is a clear relation between strain and AE energy released, assuming high strain is caused by fracturing it can be assumed that an increase in size or number of cracks is related to an increase of the cumulative amplitude recorded. More recently Lin et al. [2019] compared acoustic emission during the propagation of cracks in brittle material with digital imaging of the fracture process zone and concluded that the maximum dissipation energy is directly proportional to the critical crack opening displacement and the tensile stress.

Both the fundamental theory of Griffith as well as recent findings such as findings by Lin et al. [2019] indicate a direct causal relationship between the energy released during fracturing and the amplitude of the associated acoustic emission. Consequently the amplitude can be considered to be a good indicator for the energy released during crack formation and a a potential indicator for the size of the crack and the crack mode. However the energy of the acoustic event at the source dissipates at a rate proportional to the distance to the transducer squared, which causes the recorded amplitude to be lower than the initial amplitude. Additionally the recorded amplitude is affected by attenuation, reflection and scattering and the surface contact of the piezoelectric transducer with the sample. These situational effects needs to be accounted for when drawing conclusions from the analysis of amplitudes.

5 EXPERIMENTAL METHOD

This chapter presents the methodology followed when performing the experiments executed with the intent of researching the occurrence of acoustic activity during the deformation of rock and the manifestation of the Kaiser Effect. Two different experiments are performed during this research; loading the rock sample to failure and cyclically loading the rock sample. This chapter discusses the apparatus used, the set-up thereof, the samples tested, the procedure followed and the method of processing the acquired data.

5.1 APPARATUS

During the experiments a combination of two primary pieces of equipment is used; the standard unconfined compressive strength set-up in combination with the Richter system. This section will explain both set ups and the application thereof.

5.1.1 The unconfined compressive strength test set up

The unconfined compressive strength test is typically used to test the unconfined compressive strength of a rock. A schematic drawing of the set up is seen on the left side of 5.1. The set-up consists of a pressure bench able to apply an axial load in a digitally controlled manner and a radial- and axial strain gauge. The data acquisition of the pressure applied and the strain is digitally recorded on a computer system.

5.1.2 The Richter system

The Richter system is a continuous data acquisition system which can record acoustic activity through the usage of piezoelectric transducers. A schematic drawing of the Richter system is given on the right side of figure 5.1. The system available at the TU Delft consists of a processing PC, a master Richter and 3 slave Richters, the parameters used during the data acquisition are defined on the master Richter which the slave Richters follow. Each Richter unit can simultaneously and in a synchronised manner sample on 4 channels at once with a maximum sampling rate of 10 MHz.

5.2 SAMPLES

The experiments are performed on cores collected from two blocks of from the Stjernoy Nepheline Syenite mine, one block assumed not to be unnaturally stressed and one block collected from a highly stressed pillar. The pillar is located on a crossing in the mine, a visulisation of the situation id given in figure 5.2. During stress measurements in the past the normal stress was found to be up to 40 MPa in the vertical direction and up to 10 MPa in the horizontal direction. Lu et al. [2006]. A visual representation of the measured stress distribution in the pillar is shown in figure 5.3

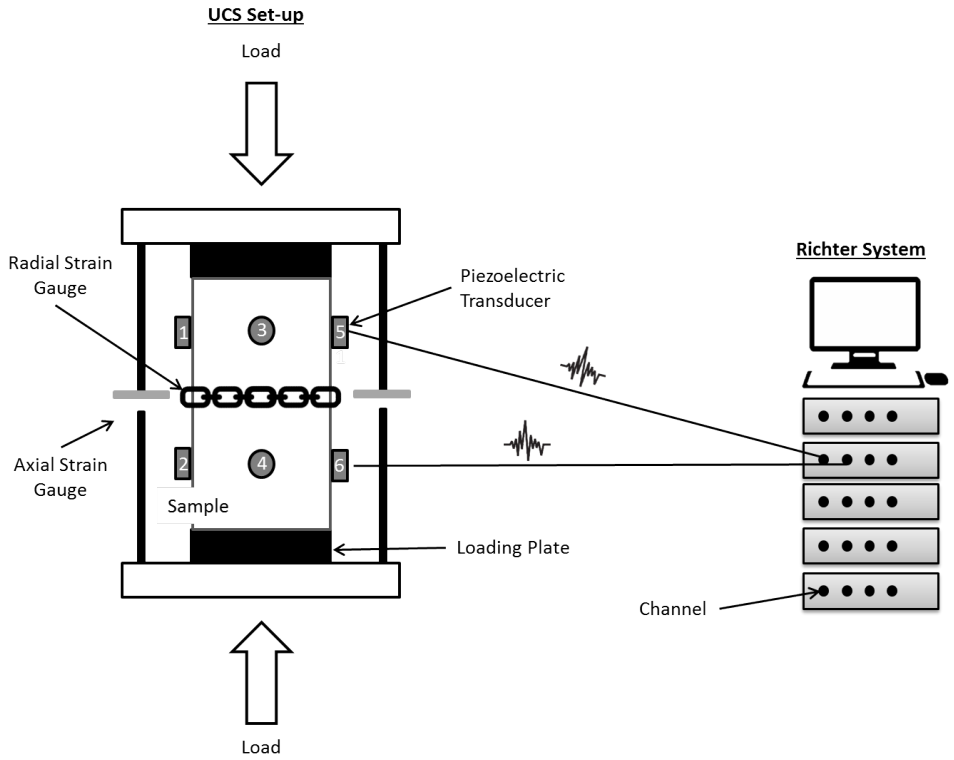

Figure 5.1: Schematic figure representing the experimental set up to collect the stress, strain data and the acoustic activity

5.3 PROCEDURE

The experiments performed during this research can be subdivided into two experimental approaches. One experiment during which the sample is loaded to failure and one experiment where the sample is loaded cyclically The geomechanical properties. Through monitoring the acoustic activity simultaneously, the concordance with the progressive deformation of the rock is obtained.

The experiments are executed with the following steps:

1 The cores are drilled with the dimensions of 60 millimetres in length and with a diameter o 30 millimetres.

2 The core is placed in a 3D printed sensory jacket with circular holes for the transducers and a slit for the radial strain gauge, as seen in figure 5.5. To record the acoustic activity throughout the experiment 6 piezoelectric transducers are attached to the sample, placed at 2 different heights and 3 different sides of the sample in a jacket.

3 The core in the sensory jacket is placed in the uniaxial compressive strength test set-up as seen in figure 5.4. The strain gauges are connected to the system controlling the UCS apparatus. The piezeoelectric transducers are connected to the Richter System.

4 Data acquisition is started for both the UCS and the Richter system

   A The acquisition of acoustic emission data is performed by the ExStream software installed on the richter system continuously at a rate of 10 MHz for all 6 channels, recording 60 million data points per second. The set-up is prepared through the steps described in the manual in the appendix.

   B The acquisition of stress and strain data is performed by the UCS system with 4 data points per second

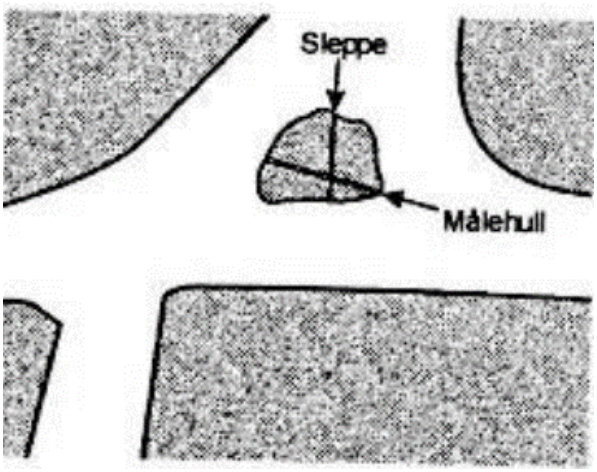

Figure 5.2: The location of the pillar in the Stjernoy mine at the crossing of four roads

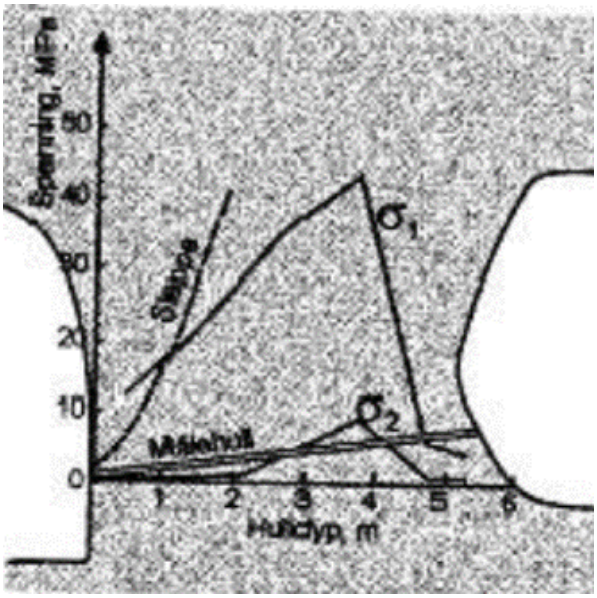

Figure 5.3: The measured stress distribution in the pillar

5 The experiment starts, the stress applied is strain (axial) controlled with a rate of 0.0001 mm/s. Either following experiment A or B

A The core is loaded to failure at once

B The core is loaded cyclically with steps of 15 MPa, returning back to a stress 5 MPa each time, up to a stress of 90 MPa after which smaller steps of 10 MPa are used up to failure.

5.4 DATA PROCESSING

The continuous acoustic data acquisition of the acoustic activity creates several gigabytes of data per minute therefore the raw data needs to be processed further to be used for analysis. Figure 4.2 visualises the full recording of a loading to failure experiment The raw data is processed by the InSite software, using an amplitude threshold based on the background noise level. InSite analyses the raw data, at the moment the amplitude recorded at two channels or more, the software takes a

Figure 5.4: Picture of the experimental set up to collect the stress, strain data and the acoustic activity

a 'snapshot' of 2048 data points the raw data for all six channels. This snapshot is stored as an acoustic event for each channel, figure 5.6 shows such an acoustic event in all 6 channels. These acoustic events are counted as 'hits', the arrival time and maximum amplitude recorded are exported and combined with the data acquired with the UCS system. This enables the researchers to relate the acoustic activity to the progressive deformation and eventual failure of the core. The data contains more information, e.g. fracture source localisation, frequency analysis, microscopy, active acoustics, i.e. velocity changes due to time limitations these possibilities were not further pursued.

Figure 5.5: Core in the 3D printed sensory jacket

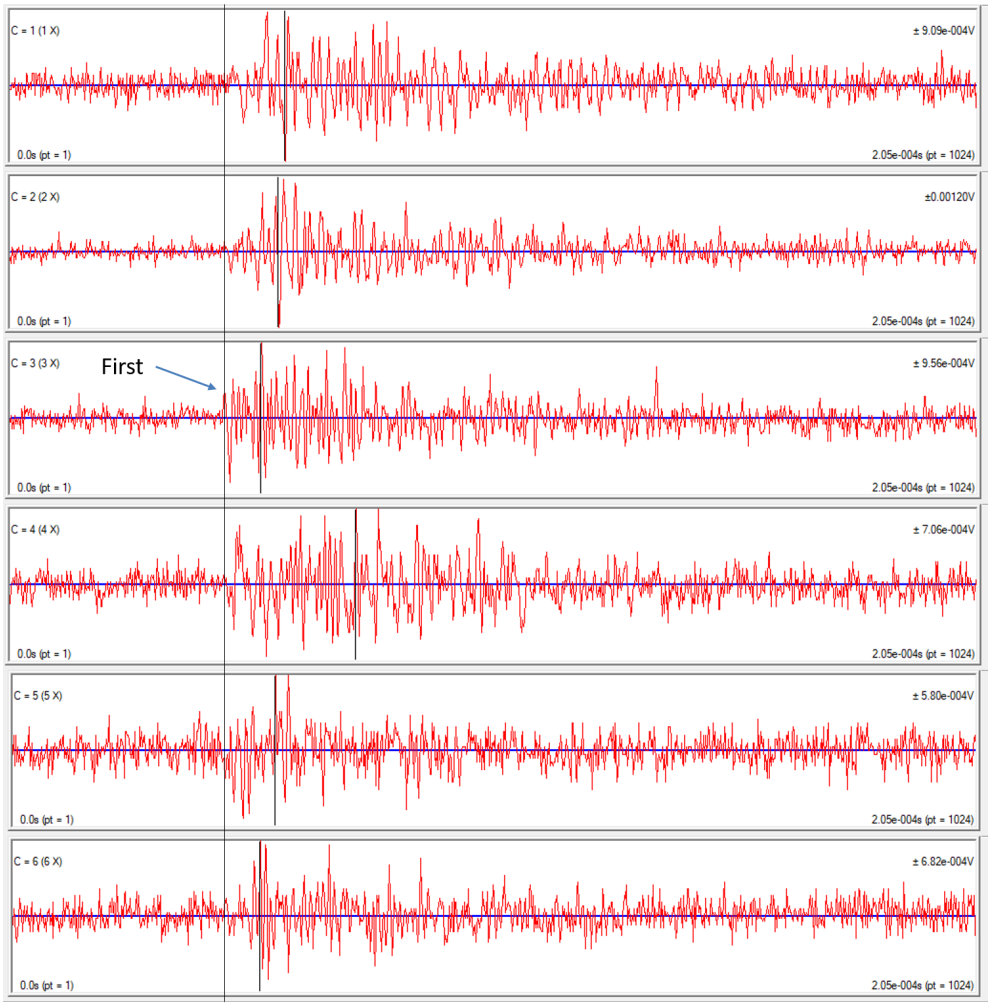

Figure 5.6: A snapshot of the continuous data triggered by an acoustic event with a line indicating the differences in arrival time

6 EXPERIMENTAL RESULTS

The results presented in this chapter are the results acquired during acoustic emission monitoring experiments in the laboratory involving loading to failure, and cyclical loading, of nepheline syenite samples received from the Stjernoya mine. The goals of the experiments are to analyse the acoustic emission during brittle deformation and relate it to physical changes within the samples, to confirm the Kaiser Effect and to explore the possibility of retrieving the in situ stress of a mine pillar in the Stjernoya mine through the Kaiser Effect. The results of the experiments can be subdivided into two categories; one category referred to as a successful experiment and the other as unsuccessful. During the unsuccessful experiments, atypical physical behaviour was observed such as chipping at the perimeter of the sample, creating a sudden substantial increase in radial strain after which it could continue to be loaded without displaying any behaviour that indicates that the sample is reaching its failure point. Since the successful experiments are considered the most representative, they are displayed and discussed in this chapter. However if the atypical geomechanical behaviour is taken into account the unsuccessful experiments display comparable behaviour regarding acoustic emission.

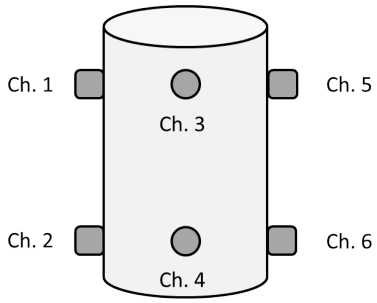

Figure 6.1: A schematic figure to clarify the location of the six sensors on the sample

6.1 AN ACOUSTIC EVENT

As discussed in the chapter 5, the data acquired by the richter system is processed using an amplitude threshold, meaning that if the threshold is exceeded, that particular instance is labelled as an event. This research is focused on the cumulative hits and the maximum amplitudes recorded during that hit. However the possibilities for analysing the event in terms of frequency, using frequency filters or using localisation algorithms to localise the sources of the acoustic events are obvious. For the sake of completeness, clarification for the potential of the set up and to demonstrate the differences of data recorded at the six sensor locations figure 5.6 visualises an event recorded at all six channels. Figure 6.1 demonstrates the location of the sensors on the sample. The amplitude ranges from 0.00058 Volt to 0.00120 Volt indicative of attenuation occurring in the sample. The location of the sensors that have recorded amplitudes of the largest difference are the furthest away from each other confirming to an extent comparable sensitivity. However the fact that even though sensor three records the wave first, the amplitude recorded is lower than that at sensor two indicates there might be a difference in sensitivity.

6.2 ACOUSTIC EMISSION CHARACTERISTICS DURING BRITTLE DEFORMATION OF GRANITE SAMPLES

Figure 6.2 visualises the geomechanical behaviour of the sample in the non cyclical experiment along with the cumulative hits recorded. For clarity the figure is plotted in a similar manner to figure 3.4 in chapter 3, the experimental results show analogous behaviour. Furthermore figure 6.3 demonstrates the development of the amplitude of recorded events as the sample is loaded.

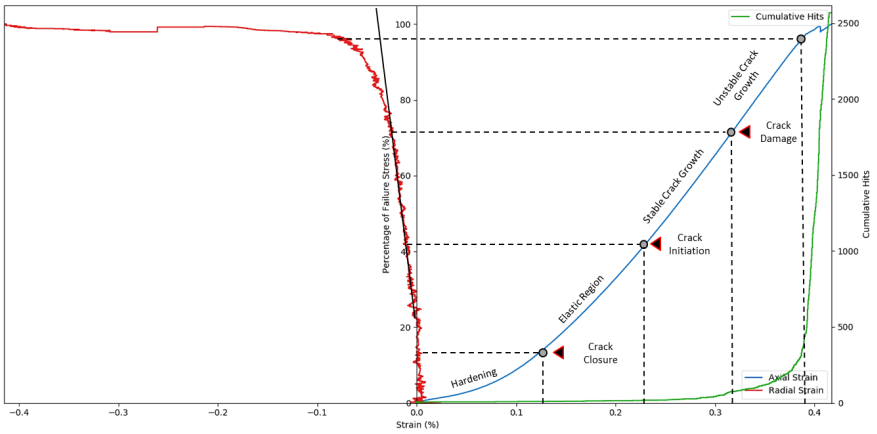

Figure 6.2: Graph visualising the axial (blue) and radial strain (red) with increasing stress and the cumulative hits (green) recorded during deformation

The initial deformation phase is a period of strain hardening and is typically referred to as a phase of crack closure. Subsequently the point at which hardening ends and the axial strain starts to exhibit linear behaviour, is commonly taken as the point at which the pre-existing cracks are closed. From this point up to crack initiation the sample is said to behave elastically, both microscopically and on a macro scale. Both during the phase of crack closure and the elastic phase limited quantities of acoustic events are recorded, never exceeding 3 percent of the total recorded events. During the phase of crack closure, the amplitudes are low, not exceeding 150 percent of the amplitude threshold. The events recorded throughout the elastic phase are typically of similarly low amplitude, however a single recorded event with a high amplitude is not exceptional.

There is a substantial increase in hits after the moment of crack initiation, as well as a significant increase of the maximum amplitudes recorded. In essence this is the phase throughout which hits with an amplitude substantially higher than the amplitude threshold appear systematically. The moment the radial strain of the sample stops behaving linearly, a phase of crack coalescence and unstable crack growth is instigated. A substantial growth in the cumulative number of hits recorded as well as a considerable rise in amplitudes of the recorded events is observed at this point. The hits recorded to this phase constitute to over 80 percent of all recorded hits. The acoustic events are clearly related to the radial deformation, indicating that microcracks initiation are mainly initiated- or propagate in the direction of the maximum compressive stress. For an overview a summary of the observations made during the loading to failure experiments is given in table 6.1.

Table 6.1: Observations made during the loading to failure experiment regarding strain, cumulative hits and the maximum amplitude per event throughout the five phases of deformation

Deformation Phase	*Axial Strain*	*Radial Strain*	*Volumetric Strain*	*Cumulative Hits (% of total)*	*Amplitude (% of noise)*
Crack Closure					
I	Linear	Linear	Compression	<1.5%, Sporadic	<150%
Elastic Region					
II	Linear	Linear	Compression	<3%, Linear	<400%, indiviual amplitudes of 1000% Systematic rise in amplitude trend & towards next phase 1000% amplitudes are the norm
Stable Crack Growth					
III	Linear	Near Linear	Compression	<25%, Systematic hits Rise in trend	
Unstable Crack Growth					
IV	Nonlinear	Nonlinear	Dilation	Exponential	Exponential rise in number of events with amplitudes of >1000%, recording amplitudes up to 3000%
Post Failure					
V	Nonlinear	Nonlinear	Dilation	Remaining	Amplitudes between 3000% and 7000% are the norm

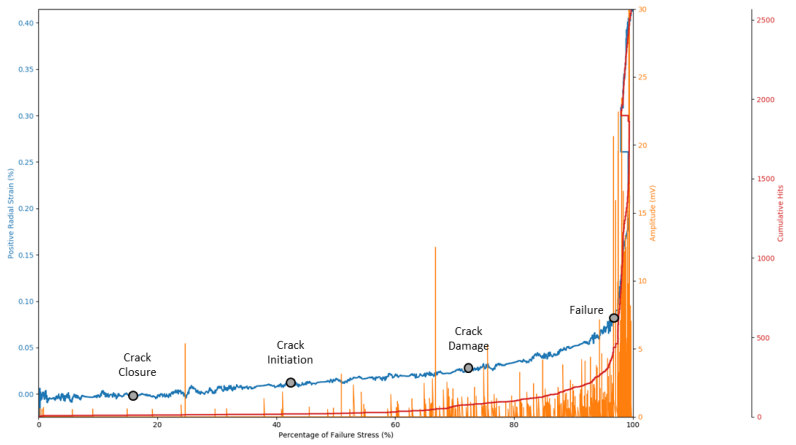

Figure 6.3: Graph visualising positive radial strain (blue), cumulative hits (red) and the maximum amplitude of each acoustic event (orange)

6.3 CONFIRMING THE KAISER EFFECT IN LAB SETTING THROUGH CYCLICAL LOADING

The Kaiser effect is the phenomenon defined as the absence of detectable acoustic emission events until the load imposed on the material exceeds the previously applied stress. One of the goals of the cyclical experiments is to confirm the occurrence of the Kaiser Effect in brittle deformation. The cumulative hits as recorded during the four cyclical loading tests are shown in figure 6.4. Samples G5 and G10 showed atypical behaviour namely chipping at the perimeter, the related jump in radial deformation is also observed in the cumulative hits recorded. Within all four experiments the Kaiser Effect can be observed to some extent however the atypical samples exhibit acoustic activity at 70 percent of maximum stress of the previous cycle, while the other samples do not exhibit acoustic activity before reaching 85 percent of the previous maximum stress. Figure 6.5 combines the radial- and axial strain and the cumulative hits for cyclical loading of sample G6 in one graph in a similar manner to figure 6.2. The cumulative hits show a relative absence of acoustic emission until the applied stress nears the stress applied during the previous cycle, essentially confirming the manifestation of the Kaiser Effect, however a clear increase in hits is observed already before reaching the maximum stress applied during the previous cycle. Since hits are not only recorded as the stress of the previous cycle is exceeded, it is concluded that the kaiser effect does not manifest perfectly.

The discrepancy in the exact overlay of cumulative hits recorded per step is similarly observed in the recorded strain. The cyclical loading causes hysteresis to occur in the sample, easily recognised in the plotted radial strain data. For the loading to failure experiments, the number of recorded acoustic events is strongly related to the radial strain. A similar effect is expected in the cyclical experiments. The imperfect manifestation of the Kaiser Effect correlates with the occurrence of hysteresis in the radial strain indicating a relationship with one another.

Previous researchers have used the felicity ratio as a measure for relating discrepancy between the onset of acoustic activity according to the Kaiser Effect and the

onset in reality. The Felicity ratio being the ratio between the stress at which the acoustic emission commences and the maximum stress previously applied. Similarly such a ratio can be found for the stress at which the onset of new radial strain occurs. These ratios are compared in 6.6. Except for an outlier during the fourth cycle the felicity ratio is between 0.85 and 0.95, where the radial strain ratio is consistently 1. The felicity ratio being lower than the radial strain confirms a relationship between the hysteresis and the acoustic events.

During the loading to failure experiments, the amplitude of the recorded events are substantially lower until the stress applied exceeds 60 percent of the peak strength. Furthermore, disregarding individual outliers, there is a clear gradual increase in the amplitude recorded. In figure 6.7 it can be observed that this is not the case for cyclical loading. High amplitudes are recorded at the full spectrum of stress applied, for the particular experiment visualised, the highest amplitude is recorded at 25 percent of the peak strength. Although high amplitude acoustic events are recorded throughout the whole scale of stresses, there is a greater abundance of high amplitudes after reaching 50 to 60 percent of the peak strength.

6.4 EXPLORING THE POSSIBILITY OF RETRIEVING THE IN-SITU STRESS THROUGH THE KAISER EFFECT

This section shows the result of the loading cores collected from a pillar in the Stjernoya mine. The sample is understood to be collected from the pillar as visualised in figure 6.8, the samples L1 and B2 are drilled in the same direction but on opposing sides of the sample and sample F3 is drilled in a direction orthogonal to F3 and B2.

The geomechanical behaviour, i.e. the strain relative to the stress and the cumulative hits of the samples of B2, F3 and L1 are visualised in figure 6.9. The radial strain of the samples B2 and F3 exhibit strong linear behaviour for the major part of the experiment. Due to grains in the radial strain chain from previous experiments, the radial strain results of the L1 sample show a lot of noise, an approximation of the actual deformation is shown in the figure. The peak strength of the three samples range from 65 MPa to 117 MPa but show similar results as obtained in previously discussed experiments. The onset of acoustic activity starts at a lower percentage of the peak strength for the samples B2 and F3 than for sample L1.

A visualisation of the development of the amplitude relative to the positive radial strain and the cumulative hits recorded are shown for the samples B2, F3 and L1 in figure 6.10, figure 6.11 and figure 6.12, respectively. The amplitudes recorded for the samples L1 and B2 show behaviour similar to that recorded in previous experiments, i.e. the amplitudes recorded at low stresses are low and gradually rise as the stress approaches the peak strength. For sample F3, the distribution of amplitude is more in concordance with the results for cyclical loading; acoustic events with high amplitudes are recorded throughout the experiment and there is not a clear trend as the peak strength is approached. However it should be noted that the amplitudes recorded during this experiment are much lower throughout the whole of the experiment and it is unclear whether this is due to reasons inherent to the sample or due to external reasons such as the sample-transducer contact.

The samples L1 and B2 are drilled in the same direction, therefore the onset of acoustic activity at the same stress would be indicative for stress memory. The pillar is an important supportive pillar and therefore it can be expected that the stress in the direction of B2 and L1 is higher than in the direction of F3 therefore an onset of acoustic activity at a lower stress than that for B2 and L1 would be indicative for stress memory. To compare the onset of acoustic emission in the three samples and check for the occurrence of the two aforementioned indicators, the cumulative hits recorded for the samples F3, B2 and L1 are combined in figure 6.13. The commencement of acoustic activity for sample F3 occurs at a far lower stress

than that of samples B2 and L1. There is an obvious difference in onset between the samples drilled in the two different directions. The onset of acoustic activity of samples B2 and L1, however, does not coincide perfectly with one another. The fact that the kaiser effect is not recognised orthogonal to the direction of the normal stres confirms findings by Stuart et al. [1993].

The change in trend of cumulative hits for L1 and B2 starts at 45 MPa, a much higher stress than the other non-stressed samples. The hits in F3 start at 20 MPa which coincides with the other tested samples. This actually agrees quite strongly with the findings of Lu et al. [2006] who found the stresses in the direction of L1 and B3 to be up to 40 MPa and the stresses in the direction of F3 to be up to 10 MPa. This is a promising finding for the application of the Kaiser effect for the retrieval of the in-situ stress field. However the samples tested are too limited to be conclusive.

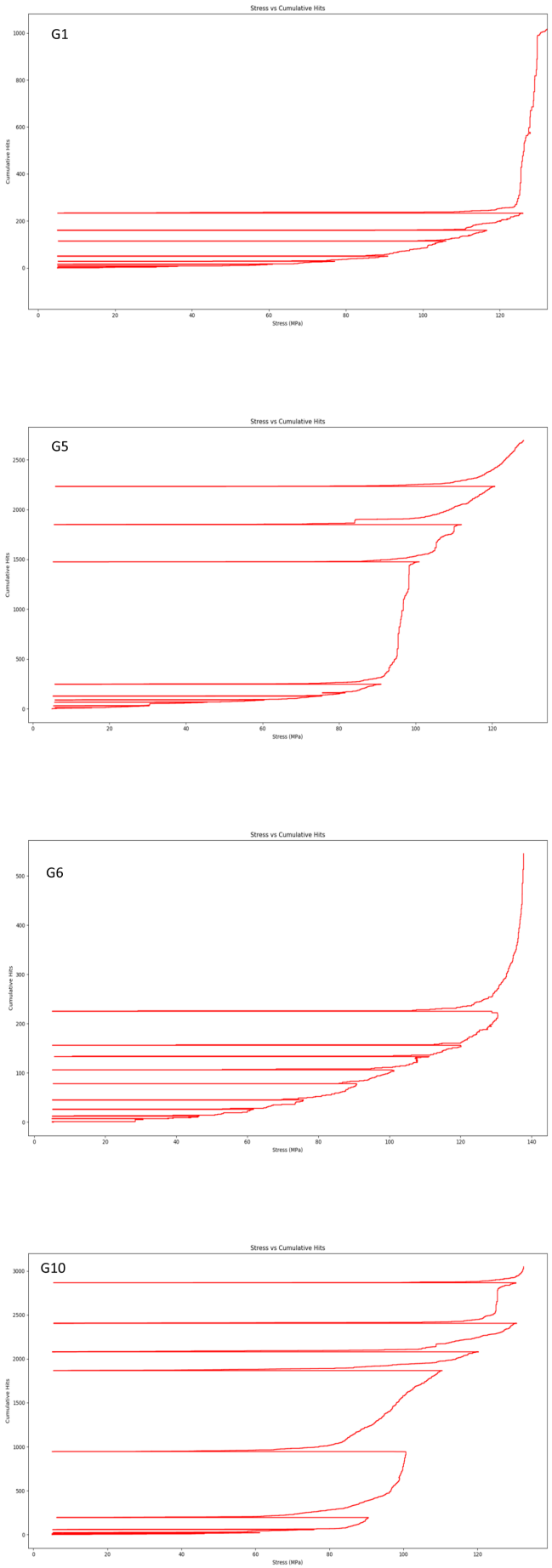

Figure 6.4: Four graphs visualising the manifestation of the Kaiser effect in sample G1, G5, G6 and G 10 during a cyclical test.

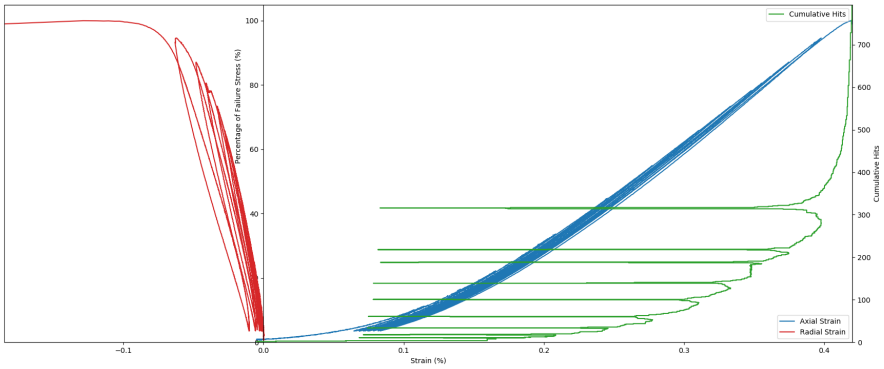

Figure 6.5: Graph visualising the behaviour of the granitic sample during cyclical loading, with strain in percentage on the x-axis, stress in MPa on the left y-axis and cumulative hits on the left y axis. The red line shows the represents radial strain, the blue line the axial strain and green line the cumulative hits

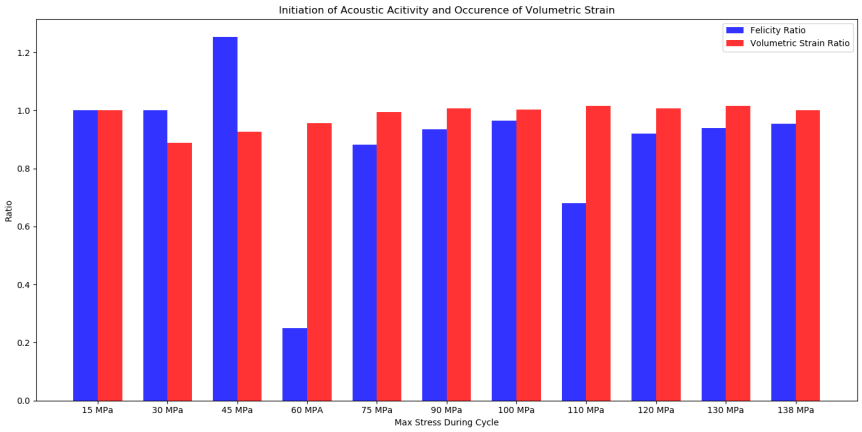

Figure 6.6: Bar graph with the blue bars visualising the stress, at which new Acoustic Events, i.e. hits are recorded, relative to the maximum stress applied during the previous cycle and the red bars visualising the stress at which a greater radial strain occurs relative to the maximum stress of the previous cycle

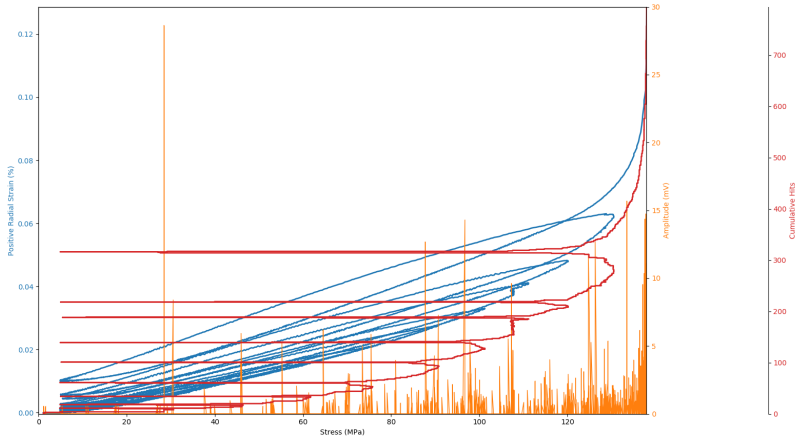

Figure 6.7: Graph visualising positive radial strain (blue), cumulative hits (red) and the maximum amplitude of each event (orange)

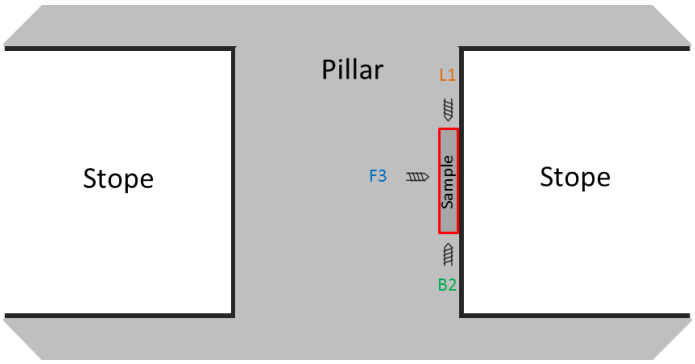

Figure 6.8: Schematic drawing of the pillar from which the samples F3, L1 and B2 are collected.

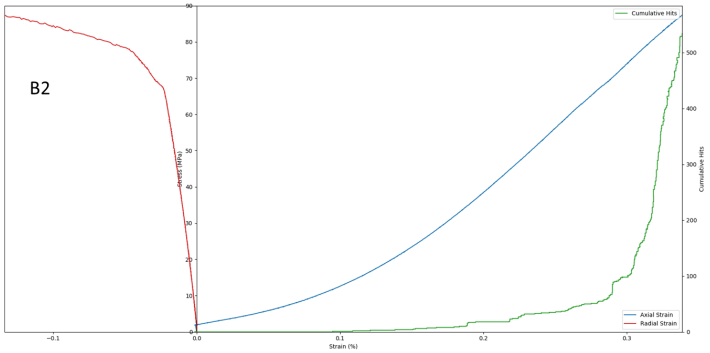

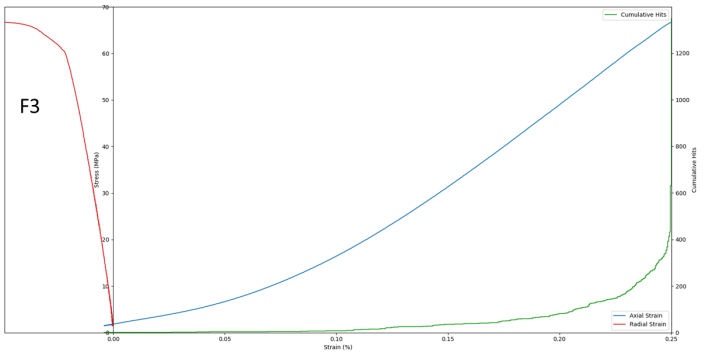

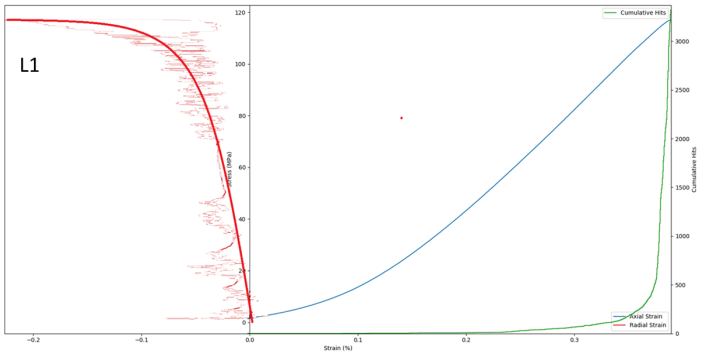

Figure 6.9: Overview of the geomechanical behaviour of sample B2, F3 and L1 respectively and the cumulative hits recorded

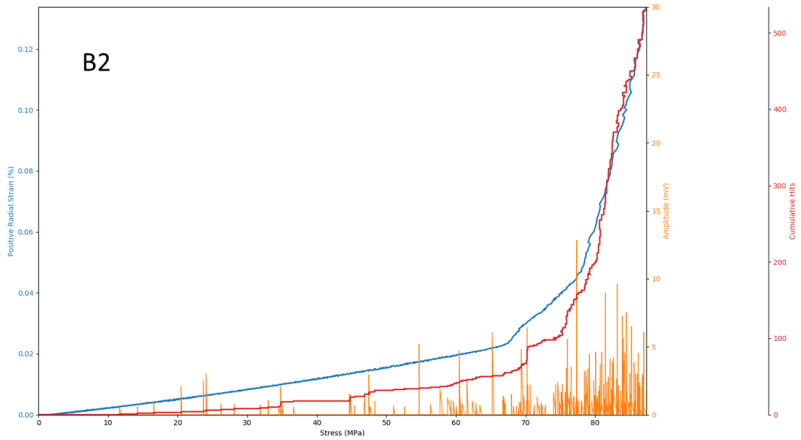

Figure 6.10: Graph visualising the number of hits recorded, the amplitude of the recorded events and the positive Radial Strain on sample B22

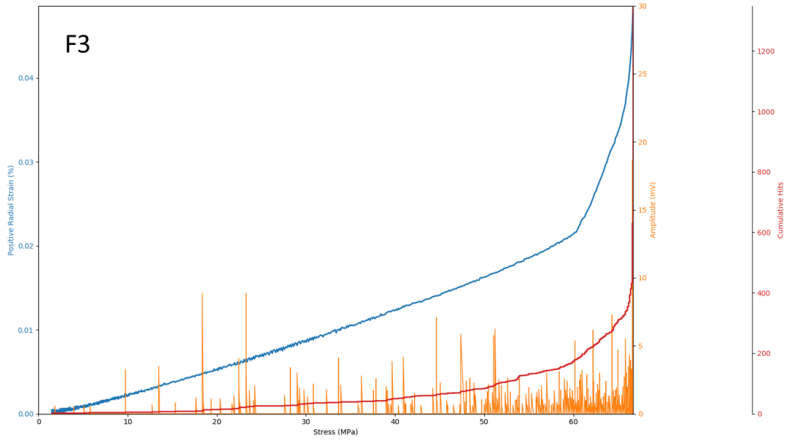

Figure 6.11: Graph visualising the number of hits recorded, the amplitude of the recorded events and the positive Radial Strain on sample F3

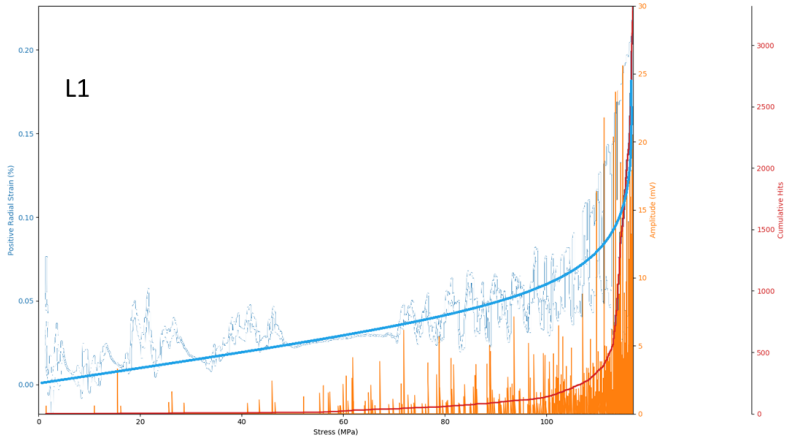

Figure 6.12: Graph visualising the number of hits recorded, the amplitude of the recorded events and the positive Radial Strain on sample L1

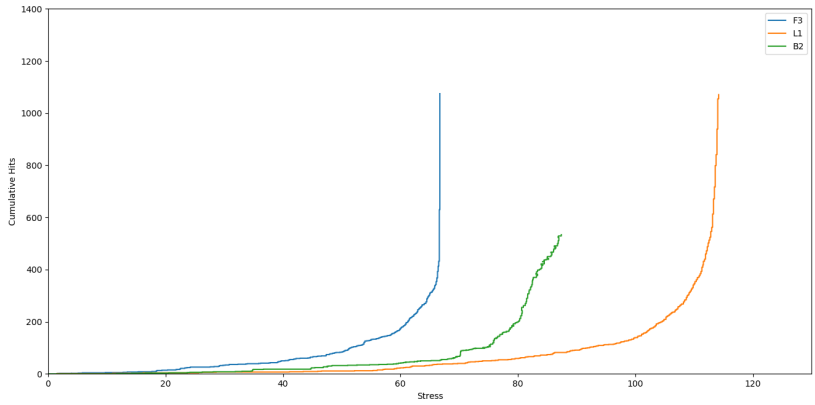

Figure 6.13: Graph visualising the recorded cumulative hits during the loading of the samples F3, L1 and B2

7 DISCUSSION

7.1 STAGES OF DEFORMATION AND ACOUSTIC EMISSION

The deformation of brittle rock has been studied by many researchers Hoek [1965], Bieniawski [1967], Brace et al. [1966], Martin [1993] gives a conclusive account of the deformation of granite and the related acoustic emission. Clearly stating the five phases of deformation. In phase I, existing cracks are closed, during phase II the rock is presumed to behave as a linear, homogeneous, elastic material. The three remaining phases being, phase III stable crack growth, phase IV unstable crack growth and phase V (post-)peak behaviour. A more detailed description of these five phases is given in chapter 3. Close to 95% of all acoustic activity occurs during the last three phases. Figure 7.1 visualises these five phases based on collected results, a schematic drawing of the crack growth in the five different stages is given under the figure.

The five different phases of deformation can all be recognised in the acoustic activity recordings to some extend. However since the number of acoustic events recorded in the phase of crack closure and the elastic phase never exceeds 3 percent of the total recorded hits, these phases are difficult to recognise. The acoustic events recorded during these phases are probably due to existing microcracks, likely from slip occurring along some of these cracks. These cracks do not follow the sliding crack model as discussed in chapter 3 as no permanent damage is recorded in the axial strain Nicksiar and Martin [2014]. The commencement of crack initiation is easier to recognise in the acoustic activity than it is in the stress-strain curve, as there is an obvious rise in the trend of the cumulative hits at that point. The crack initiation is found to be between 40% and 55% of the uniaxial compressive strength similar to early work of Brace et al. [1966] and Bieniawski [1967] and confirmed through acoustic emission monitoring by Nicksiar and Martin [2013], Nicksiar and Martin [2014] and Eberhardt et al. [1998]. The moment of crack coalescence, i.e. the transition to phase four is similarly clear; the trend of the cumulative hits moves from relatively linear to an exponential increase in hits. This typically occurs between 75% and 85% of the uniaxial compressive strength. Similar findings through acoustic emission monitoring have been done by Martin et al. [1999]. Lockner et al. [1991] showed using localised acoustic events that the abrupt increase in cumulative hits is due to the move from uniformly distributed individual cracks to crack coalescence starting on the boundary of the sample, then spreading through the sample. The crack coalescence as a source for the abrupt increase in cumulative acoustic emission is confirmed by Diederichs et al. [2004]'s discrete element simulation approach; first showing uniform distribution of cracks, the onset of interaction and finally macro fractures from boundary to boundary

Further analysis of the characteristics of the acoustic events often focuses on the frequency-magnitude relation for acoustic emission events or the Gutenberg-Richter b-value relation for earthquakes. This research however focuses on the amplitude of the wave. Unlike the number of hits recorded, the rising trend of the amplitude, as the deformation transcends through the five phases has not been researched extensively. The amplitude is strongly dependent on scattering and attenuation and both are dependent on the material and geometry of the sample. Furthermore the surface contact of the piezoelectric transducers and the sample strongly affects the amplitude recorded. As stated in chapter 6 there are differences in the amplitude

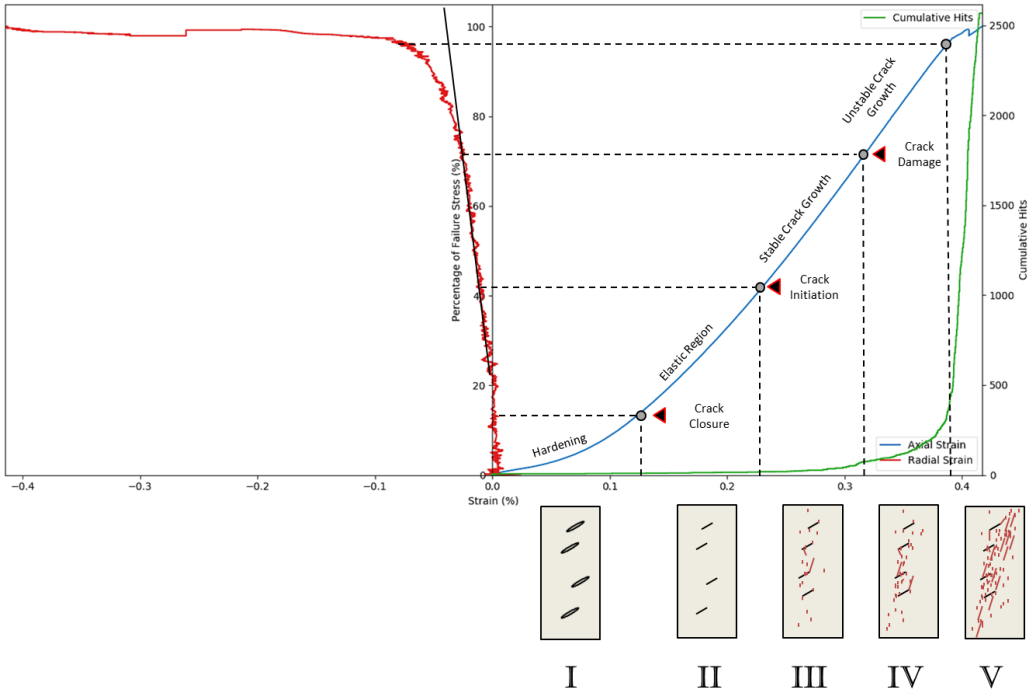

Figure 7.1: Result based visualisation of the radial behaviour and acoustic behaviour in terms of hits during deformation, including a schematic drawing of the growth of microcracks during the five phases of deformation, based on Martin [1993] and Cai et al. [2004]

of the wave reaching the sensors that may indicate a difference in sensitivity. Additionally the individual events may have an amplitude tenfold of the nearby events, therefore individual events should not be used as indicator for the damage in the rock but the overall trend or the total amplitude can be. So although analysing the change in amplitude during the different phases of deformation is not as definitive as the cumulative hits, there is an obvious rising trend of the amplitude as the deformation transcends from one phase to the next. The similarity of the findings of this research with the findings of Martin [1994], Hoek and Martin [2014] are recognised easily looking at figure 1.1 in chapter 1 and figure 6.2 in 6.

Additional to the possibility of seeing a reflection of the five phases of deformation in the acoustic activity recorded. There is a strong correlation between the radial deformation and the cumulative hits recorded in combination with the gradual increase of high amplitude events as the stress rises imply that the microcracks form and propagate mainly parallel to the compressive stress. These findings are similar to findings by Brace et al. [1966] regarding dilatancy during compression- and by Martin [1994] in the progressive fracturing of Lac Du Bonnet granite. The main models for crack initiation the sliding crack model and the force-chain crack model would exhibit this behaviour on macro scale. Similar behaviour is observed in the formation of cracks in mine pillars, in these mine pillars deformation occurs in such a way that the mine pillar starts to exhibit what is sometimes called onion-skin as it it moves from having near orthogonal walls to concave walls that develop due to fractures forming parallel to the main stress on the pillar which is usually orthogonal to roof the pillar carries.

Throughout the experiments during which the sample is loaded to failure at once, there is an obvious trend of an increasing amplitude in the experiments. During the phase of crack closure, the amplitude does not exceed 150 percent of the amplitude threshold. During the elastic phase one or two events of 10 times the amplitude threshold are observed but generally do not exceed 300 percent of the threshold.

7.2 CYCLICAL LOADING AND THE KAISER EFFECT

Cyclical stressing of rocks changes the elastic moduli, the crack damage of the rock, decreases the shear strength of joints Haimson [1978] Jing et al. [1993] Heap et al. [2009] researched the effect the change in elastic moduli had on the acoustic emission and found that there is no change in the moduli if there is no acoustic emission recorded. However the amplitude change during the cyclical stressing relative to non cyclical stressing, i.e. loading to failure is not discussed. During the loading to failure experiments an obvious rise in the trend of the amplitudes recorded is observed as the rock approaches failure. However the trend in amplitude is more ambiguous throughout the cyclical experiments. Several causes of this phenomenon can be thought of; firstly considering Griffith's crack model it is possible that the cyclical loading has decreased the strain energy that needs to be overcome for cracks to initiate and propagate. Secondly considering the stable crack growth between 40 and 70 percent of the peak strength and unstable crack growth approaching peak strength, it can be assumed that if the sample is unloaded after surpassing 70 percent of the peak strength, unstable crack growth may occur at lower stresses. Thirdly since it is found that the force-chain crack model accurately describes the initiation and propagation of crack growth up to 60 to 70 percent of peak stress after which crack growth is more accurately described by the sliding crack model it could be the case that may be the cause of recording acoustic events with the characteristics usually associated with cracks formed at higher stresses. However no research has been done that links the high amplitude acoustic events with the sliding crack model and low amplitudes with the force-chain crack model.

The Kaiser effect is confirmed to some extent in all cyclical lab experiments. In a review written by Lavrov [2003] on the Kaiser effect, similar occurrences of the Kaiser Effect with similar Felicity Ratios are discussed. Reviews of Holcomb [1993] and Lockner [1993] express similar findings. However in the same review it is also stated that it is not possible to use the Kaiser effect to determine the full in-situ in stress tensor. It is stated that at best it is possible to estimate the linear combination of in-situ stresses, when testing the sample oriented exactly in the direction of the normal in situ stress. The reason for this is a combination of the loss of the Kaiser Effect if the stress applied deviates more than 10 degrees from the direction of the stress being recovered and the fact that the triaxial stresses occurring in situ are not simulated during the uniaxial testing. The results of the experiments performed on the samples collected from the pillar reflect these findings, the onset of acoustic emission is the same for sample L1 and B2 but different for the sample F3 drilled in a different direction. However it is not known what the direction of the main stress is so therefore it is not known whether the stresses found describe the normal stress.

7.3 PRACTICAL IMPLICATIONS

Monitoring in the earth sciences is used to predict unwanted effects in terms of rock failure such as rockbursts in mine pillars and tunnels, breakouts in boreholes or the occurrence of landslides and earthquakes. The fact that the different phases of deformation are recognised so well in the acoustic activity have positive implications for in situ monitoring. The trend of the cumulative hit recorded can be used to determine whether the rock is approaching failure, this finding is helpful for analysing in situ scenarios as the cumulative hits can be used as a tool for approximating the proximity to failure.

Additionally it is observed in the lab that if the sample is loaded to failure at once, there is an obvious rise in amplitudes as the sample transcends through the phases of deformation and approaches failure. The amplitude is not as straightforward

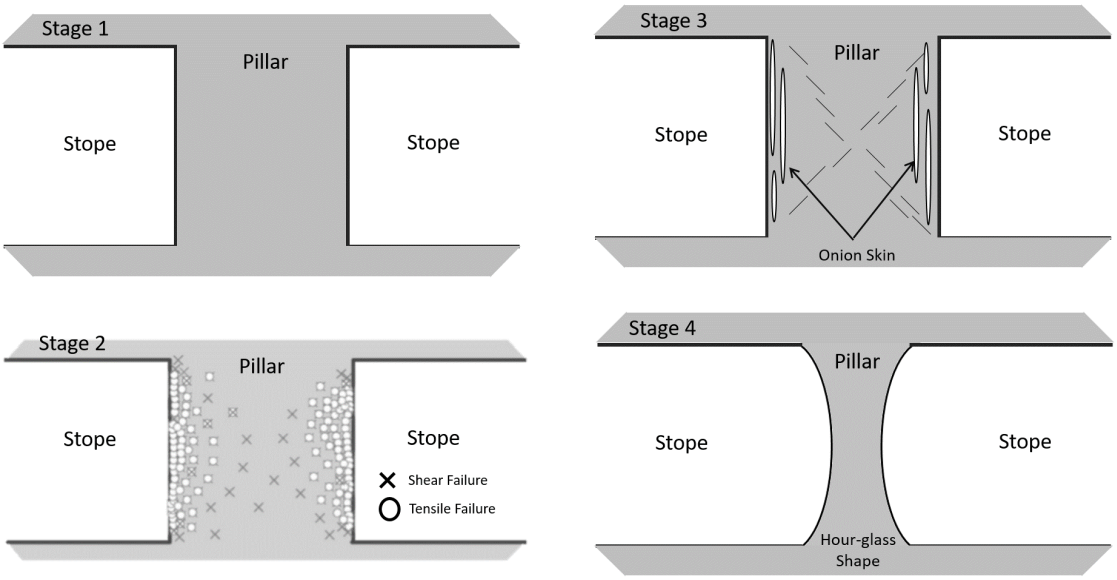

Figure 7.2: Progressive pillar failure including the findings of Martin [2000] regarding tensile and shear failure in a mine pillar. The progressive failure ends in the typical hour glass shape of a failed mine pillar

to use for tracking the deformation due to singular high amplitude events at low stresses, it could however be used as a predictive method for high energy events in the earth sciences. In the lab it is shown that if a sample is loaded cyclically, amplitudes typical for stress above 60 percent of the peak strength are recorded throughout the loading cycle starting around 20 percent of the peak strength. This implies that high energy releases occur at low stresses after a rock has been loaded to a stress approaching peak stress. An implication of this could be that during the reloading a mine pillar, borehole or landmass at angle after it has been unloaded, high energy acoustic events, such as rockbursts, outbreaks or landslides may occur at lower stresses than anticipated.

Specifically regarding failure in mine pillars it has been shown that the dominant mode of failure is the formation of microcracks progressing into slabbing and spalling Martin [2000] creating the typical hour glass figure. A Schematic drawing of the progression of a mine pillar failure is shown in figure 7.2.

The experiments performed on the samples collected from the mine pillar indicate that the Kaiser Effect also occurs to some extent in situ. It has been shown by many researchers that the Kaiser effect cannot be used to retrace the in situ stress through uniaxial reloading in the lab Lavrov [2003]. However the Kaiser Effect may have implications for monitoring. In case of monitoring a rock mass that is reloaded after it has been loaded to a stress beyond the crack initiation stress of the rock, a relative silence in terms of acoustic activity is implies that the stress applied is not nearing the maximum previously applied stress.

8 CONCLUSION

8.1 CONCLUSION

- It is possible to acquire enough acoustic data with the Richter system in the set up described in this thesis to recognise the different phases of deformation as described by Martin Nicksiar and Martin [2014].

- Additional to the cumulative hits the maximum amplitude of the events recorded has shown to correspond to damage in the rock as well. During the loading to failure experiments a clear rise in the trend of the maximum amplitudes is observed as the rock nears failure. In general no amplitudes higher than 300% of the noise level are recorded before crack initiation is reached (around 45% of the peak stress), after which the trend progresses from linear to exponential as the sample nears failure. The amplitudes of individual events cannot be used as an indicator for the damage in the rock, since individual events incidentally have much higher amplitudes than its surrounding events. During the cyclical loading experiments the trend is far less clear as amplitudes of 1000% occur already at 25% of the peak strength indicating that the mode of fracturing that is typical for near failure stresses is occurring at low stresses. The in-situ implications of high amplitudes at low stress can be that fracturing related events such as rock bursts, earthquakes or landslides may occur at much lower loads than anticipated.

- During cyclical loading of the samples, a near silence in terms of acoustic hits was observed until nearing the previous maximum stress. Often however a substantial number of hits were recorded at around 85% of the previously applied stress. It can concluded that the Kaiser Effect does occur but that it does not manifest perfectly.

- Three samples collected from a heavily stressed mine pillar in the Stjernoya mine showed behaviour resembling the Kaiser effect. The two samples collected in the direction of the normal stress exhibited acoustic activity at a higher stress than the sample collected orthogonal to the normal stress. The stress at which the acoustic activity starts may be indicative of the in-situ stress in the mine. To the very least it can be said that the difference in on set of acoustic activity in the two directions show that acoustic activity corresponds to some extent to the stress in the pillar. These findings are promising for the use of acoustics as an indicative measure for pillar failure or rock burst prediction.

- For future work in the lab it is recommended to use a combination of fracture source localisation, frequency analysis, microscopy, active acoustics, i.e. velocity changes, CT scanning and chemical analysis of the healing, loading-unloading hysteresis and closing process of cracks on a range of rocks to develop a better understanding of the fracture modes during stable crack growth, unstable crack growth and post failure behaviour. The implications of the outcome would range from improving the understanding of the fundamentals of fracture mechanics to improvement of the rock monitoring applied to a large range of applied earth science applications.

- The observation that amplitudes typical for high stresses (70% peak stress) are recorded at low stress (25% of peak stress) may imply that similar behaviour occurs on a large scale in rockbursts or earthquakes. Cyclical loading under triaxial stress conditions, as a more representative experiment, should be performed for a further understanding.
- To use acoustics as a monitoring method for pillar failure, rockburst prediction and the prediction of seismic activity in a mine. In-situ monitoring needs to be performed to examine the agreement with the findings in the lab and the effect of noise from the mining activities on the practicality of this monitoring method.

BIBLIOGRAPHY

Atkinson, B. (1987). Academic Press Inc. Ltd., London.

Baud, P. and Meredith, P. (1997). Damage accumulation during triaxial creep of darley dale sandsone from pore volumometry and acoustic emission. *International Journal of Rock Mechanics and Mining Sciences*, 34:3-4.

Bieniawski, Z. (1967). Mechanism of brittle fracture of rock, parts i, ii, and iii. *International Journal of Rock Mechanics and Mining Sciences*, 4:395–406.

Brace, W., Paulding, B. J., and Scholz, C. (1966). Dilatancy in the fracture of crystalline rocks. *Journal of Geophysical Research*, 71 - No. 16:256–272.

Cai, M., Kaiser, P.K., Tasaka, Y., Maejima, T., Morioka, H., and Minami, M. (2004). Generalized crack initiation and crack damage stress thresholds of brittle rock masses near underground excavaions. *International Journal of Rock Mechanics Mining Sciences*, 41:833–847.

Costin, L. (1983). A microcrack model for the deformation and failure of brittle rock. *Journal of Geophysical Research*, 88:9485–9492.

Cox, S. and Meredith, P. (1993). Microcrack formation and material softening in rock measured by monitoring acoustic emissions. *International Journal of Rock Mechanics and Mining Sciences Geomechanics Abstracts*, 30:11–24.

Diederichs, M., Kaiser, P., and Eberhardt, E. (2004). Damage initiation and propagation in hard rock during tunnelling and the influence of near-face stress rotation. *International Journal of Rock Mechanics and Mining Sciences*, 41(5):785–812.

Eberhardt, E., Stead, D., Stimpson, B., and Read, R. (1998). Identifying crack initiation and propagation thresholds in brittle rock. *Canadian Geotechnical Journal*, 35(2):222–233.

Griffith, A. (1920). The phenomena of rupture and flow in solids. *Philosophical Transactions of the Royal Society of London, Series A. Mathematical and Physical Sciences*, 221 (587):713–726.

Haimson, B. (1978). Effect of cyclic loading on rock. *American Society for Testing and Materials*, 654:228–245.

Hardy, H. (2005). *Acoustic emission/microseismic activity: volume 1: principles, techniques and geotechnical applications*. A.A. Balkema Publishers, 1 edition.

Heap, M., Vinciguerra, S., and Meredith, P. (2009). The evolution of elastic moduli with increasing crack damage during cyclic stressing of a basalt from mt. etna volcano. *Tectonophysics*, 471:153–160.

Heimisson, E., Einarsson, P., Sigmundsson, F., and Brandsdottir, B. (2002). Kilometer-scale kaiser effect identified in krafla volcano, iceland. *Geophysical Research Letters*, 39:7958–7965.

Hoek, E. (1965). Rock fracture under static stress conditions. CSIR Report MEG 383, National Mechanical Engineering Research Institute. Pretoria, South Africa.

Hoek, E. and Martin, C. (2014). Fracture initiation and propagation in intact rock - a review. *Journal of Rock Mechanics and Geotechnical Engineering*, 6:287–300.

Holcomb, D. (1993). A microcrack model for the deformation and failure of brittle rock. *International Journal of Rock Mechanics and Mining Sciences Geomechanics Abstracts*, 30:929–935.

Holcomb, D. and Costin, L. (1986). Detecting damage surfaces in brittle materials using acoustic emissions. *Journal of Applied Mechanics*, 53:536–544.

Hu, X., Su, G., Guanyan, C., Shiming, M., Feng, X., Mei, G., and Huang, X. (2018). Experiment on rockburst process of borehole and its acoustic emission characteristics. *Rock Mechanics and Rock Engineering*, 52 (3):783–802.

Hughson, D. and Crawford, A. (1986). Kaiser effect gauging: A new method for determining the pre-existing in-situ stress from an extracted core by acoustic emissions. In *Proceedings of the International Symposium on Rock Stress and Rock Stress Measurements, 1-3 Septemer, Stockholm, Sweden*.

Inglis, C. (1913). Stresses in a plate due to the presence of cracks and sharp corners. *Transactions of the Institute of Naval Architects*, 55:219–242.

Ishida, T., Labuz, J., Manthei, G., Meredith, P., Nasseri, M., Shin, K., Yokoyama, T., and Zang, A. (2017). Isrm suggested method for laboratory acoustic emission monitoring. *Rock Mechanics and Rock Engineering*, 50:665–674.

Jing, L., Stephansson, O., and Nordlund, E. (1993). Study of rock joints under cyclic loading conditions. *Rock Mechanics and Rock Engineering*, 26 (3):215–232.

Kaiser, J. (1950). *An Investigation into the Occurrence of Noises in Tensile Tests or a Study of Acoustic Phenomena in Tensile tests*. PhD thesis, University of Manitoba, Winnipeg.

Kallimogiannis, V., Saroglou, H., and Tsiambaos, G. (2017). Symposium of the international society of rock mechanics. In *Procedia Engineering*, pages 1108–1116.

Kranz, R. (1983). Microcracks in rocks: a review. *Tectonophysics*, 100 (B3):449 – 480.

Lavrov, A. (2003). The kaiser effect in rocks: principles and stress estimation techniques. *International Journal of Rock Mechanics Mining Sciences*, 40:151–171.

Lawn, B. (1993). Press Syndicate of the University of Cambridge, 2 edition.

Lehtonen, A., Cosgrove, J., J.A., H., and Johansson, E. (2012). An examination of in situ rock stress estimation using the kaiser effect. *Engineering Geology*, 124:24–37.

Li, B., Goncalves da Silva, B., and Einstein, H. (2019). Laboratory hydraulic fracturing of granite: Acoustic emission observations and interpretation. *Engineering Fracture Mechanics*, 209:200–220.

Li, C. and Nordlund, E. (1993). Experimental verification of the kaiser effect in rocks. *Rock Mechanics and Rock Engineering*, 4:333–351.

Lin, Q., Wan, B., Yan, W., Lu, Y., and Labuz, J. (2019). Unifying acoustic emission and digital imaging observations of quasi-brittle fracture. *Theoretical and Applied Fracture Mechanics*, 103.

Lockner, D. (1993). The role of acoustic emission in the study of rock. *International Journal of Rock Mechanics and Mining science Geomechanics Abstracts*, 30 (7):883–899.

Lockner, D., Byerlee, J., Kusenko, V., Ponomaarev, A., and A., S. (1991). Quasi-static fault growth and shear fracture energy in granite. *Nature*, 350:39–42.

Loutas, T. and Kostopoulos, V. (2009). Health monitoring of carbon/carbon, woven reinforced composites. damage assessment by using advanced signal processing techniques. part i: Acoustic emission monitoring and damage mechanisms evolution. *Composites Science and Technology*, 69 - issue 2:256–272.

Lu, M., Li, C., Kjorholt, H., and Dahle, H. (2006). In *In-Situ Rock Stress: International Symposium on In-Situ Rock Stress, Trondheim, Norway*, pages 19–21.

Martin, C. (1993). *The Strength of Massive Lac du Bonnet Granite Around Underground Openings*. PhD thesis, University of Manitoba, Winnipeg.

Martin, C. (1994). The progressive fracture of lac du bonnet granite. *International Journal of Rock Mechanics Mining Sciences and Geomechanics*, 31:643–659.

Martin, C., Kaiser, P., and McCreath, D. (1999). Hoek-brown parameters for predicting the depth of brittle failure around tunnels. *Canadian Geotechnical Journal*, 36:136–151.

Martin, C.D.and Maybee, W. (2000). The strength of hard-rock pillars. *International Journal of Rock Mechanics Mining Sciences*, 37:1239–1246.

Mclaskey, G., Glaser, S., and Grosse, C. (2010). Beamforming array techniques for acoustic emission monitoring of large concrete structures. *Journal of Sound and Vibration*, 329:2384–2394.

Michihiro, K., Yoshioka, H, and Fujiwara, T. (1991/1992). The kaiser effect in rocks: principles and stress estimation techniques. *Journal of Acoustic Emission*, 10(1-2):S63–S76.

Momayez, M. and Hassuni, E. (1992). Application of kaiser effect to measure in-situ stresses in underground mines. In *The 33rd U.S. Symposiumn on Rock Mechanics (USRMS), 3-5 June, Santa Fe, New Mexico*.

Nicksiar, M. and Martin, C. (2013). Crack initiation stress in low porosity crystalline and sedimentary rocks. *Engineering Geology*, 154:64–76.

Nicksiar, M. and Martin, C. (2014). Factors affecting crack initiation in low porosity crystalline rocks. *Rock Mechanics and Rock Engineering*, 47:1165–1181.

Pappas, Y., Markopoulos, Y., and Kostopoulos, V. (1998). Failure mechanisms analysis of 2d carbon/carbon using acoustic emission monitoring. *NDT E International*, 31 - issue 3:157–163.

Sayers, C. and Kachanov, M. (1995). Microcrack-induced elastic wave anisotropy of brittle rocks. *Journal of Geophysical Research*, 100 (B3):4149–4156.

Sheng, M., Tian, S., zhang, B., and Hangkui, G. (2019). Frequency analysis of multi-sources acoustic emission from high-velocity waterjet rock drilling and its indicator to drilling efficiency. *International Journal of Rock Mechanics and Mining Sciences*, 115:137–144.

Stuart, C., Meredith, P., Murrel, S., and Van Munster, J. (1993). Anisotropic crack damage and stress-memory effects in rocks under triaxial loading. *International Journal of Rock Mechanics and Mining Sciences Geomechanics Abstracts*, 30:937–941.

Thompson, B., Young, R., and Lockner, D. (1999). Fracture in westerly granite under ae feedback and constant strain rate loading: Nucleation, quasi-static propagation and the transition to unstable fracture propagation. *Pure and Applied Geophysics*, 36:995–1019.

Villaescusa, E., Seto, M., and Baird, G. (2002). Stress measurements from oriented core. *International Journal of Rock Mechanics Mining Sciences*, 39:603–615.

Young, P. and Martin, C. (1993). Potential role of acoustic emission/microseismicity investigations in the site characterization and performance monitoring of nuclear waste repositories. *International Journal of Rock Mechanics and Mining Sciences Geomechanics Abstracts*, 30 - issue 7:797–803.

Zang, A., Wagner, C., and Dresen, G. (1996). Acoustic emission, microstructure, and damage model of dry and wet sandstone stressed to failure. *Journal of Geophyscal Research*, 101-B8:17507–17521.